The Leon 1: A 3D Printed Liquid Methane/Liquid Oxygen Pressure-FED Rocket Propulsion System

A project present to
The Faculty of the Department of Aerospace Engineering
San Jose State University

in partial fulfillment of the requirements for the degree
Master of Science in Aerospace Engineering

By

Andres J. Masterman

May 2015

approved by
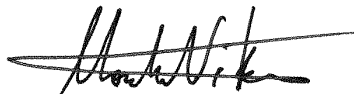
Dr. Nikos Mourtos
Faculty Advisor

San José State
UNIVERSITY

The Designated Project Committee Approves the Project Titled

THE LEON 1: A 3D PRINTED LIQUID METHANE/LIQUID OXYGEN PRESSURE-FED
ROCKET PROPULSION SYSTEM

by Andrew J. Masterman

APPROVED FOR THE DEPARTMENT OF AEROSPACE ENGINEERING

SAN JOSÉ STATE UNIVERSITY

May 2015

Dr. Nikos Mourtos   Department of Aerospace Engineering

Dr. Periklis Papadopuolos   Department of Aerospace Engineering

Dr. Kamran Turkoglu   Department of Aerospace Engineering

ABSTRACT

Methane propulsion, until most recently, has been a relatively untapped resource. But with increasing interest in sending humans to the planet Mars, its use in a rocket propulsion system has gone under more study. Its cost, energy density, and manufacturability from the Martian atmosphere make it the most popular choice for such a system. Additionally, for increased simplicity and reliability, a descent or ascent stage for a piloted Martian spacecraft will almost certainly contain a pressure-fed engine cycle. This paper details the background, engineering principles, and preliminary design of such a system, intended to be 3D printed to demonstrate the practice of rapid prototyping. Designed with undergraduate senior Michael Bell, the Leon-1 is San Jose State University's first 3D printed liquid bipropellant rocket engine that is also geared towards the development of the fuel combination using liquid oxygen (LO2) and liquid methane (LCH4) for Mars mission applications. The project was designed using original calculations, coupled with computer simulations from Rocket Propulsion Analysis (RPA), SolidWorks, and ESI.

TABLE OF CONTENTS

NOMENCLATURE

a   = Local speed of sound (ft/s), stoichiometric coefficient

A_e= Nozzle exit area, in^2

A_t= Nozzle throat area, in^2

b   = Assigned mass of compound (g/mol)

BTU   = British Thermal Unit

c*   = Characteristic Velocity, ft/s

c   = Effective exhaust velocity, ft/s

C_f= Thrust Coefficient

CFD   = Computational Fluid Dynamics

C_p = Specific heat at constant pressure, Btu/lb-°R

D   = hydraulic diameter, ft

d   = bulk density or the propellant combinations specific weight

d_e= Equivalent diameter of the coolant passage

$d\dot{m}_f$= rate of the coolant vaporization

F= Thrust, lbf

g= Gravitational constant, ft/s^2

h= Heat transfer coefficient, Btu/(ft^2 s °R)

h_c= Coolant-side-heat transfer coefficient, Btu/ft^2-h

h_g= Gas-side-heat transfer coefficient, Btu/ft^2-h

= Enthalpy, J/mol

I_{sp}= Specific Impulse, s

J= Energy Conversion Factor, ft-lb/Btu

k= gas thermal conductivity, Btu/h-ft^2-°R/ft

L*   = Combustion chamber characteristic length, in

L_c = Combustion chamber length, in

L_n = Nozzle Length, in

LO_2 = Liquid Oxygen

LCH_4 = Liquid Methane

$\dot{m}$ = mass flow rate, lbm/s

$\dot{m}_f$ = mass flow rate of the coolant in the film, lbm/s

$\dot{W}$ = Steady weight flow rate, lb/s

M   = Molecular weight of combustion products

M_e= Nozzle exit Mach

M_x= Local Mach Number

P_a= Atmospheric pressure, lbf/in^2

P_{cns}= Nozzle stagnation pressure or chamber total pressure, lbf/in^2

P_e= Nozzle exit pressure, lbf/in^2

Pr   = Prandtl Number, $\mu C_p/k$

P_t = Nozzle throat pressure, lbf/in^2

q   = Heat flux, Btu/(ft^2 s)

q_r = Radiation heat flux, Btu/(ft^2 s)

Q = Thermal energy/Heat flow rate, Btu/s

R   = Contour circular arc, in; Nozzle radius of curvature at throat, ft

R*   = Universal gas constant, in-lbf/slug °R

R_a = Arithmetic mean of surface roughness

R_t = Nozzle throat radius, in

SA_c = Combustion chamber surface area

T = Temperature, °R

T_o = Stagnation Temperature, °R

T_{aw} = Adiabatic wall temperature of the gas, °R

T_c = Chamber pressure, psi

T_e = Nozzle exit temperature, °R

T_t = Nozzle throat temperature, °R

T_{wg} = Hot-gas-side local chamber-wall temperature, °R

T_{wc} = Coolant side local chamber-wall temperature, °R

V_c = Combustion chamber volume, in^3

 = Internal energy, J/mol

v_e = Exhaust velocity, ft/s

α = Conical nozzle half-angle, degrees

γ = Specific heat ratio

ΔS = Change in Entropy, Btu/°R

ϵ = Nozzle expansion ratio

ϵ_c = Nozzle contraction area ratio

ε_e = effective emissivity coefficient of the wall

ε_w = effective emissivity coefficient of the wall material

ε_r^T = effective emissivity coefficient of the reaction products at temperature T_{aw}

η_f = Correction factor for thrust and the thrust coefficient

η_v = Correction factor for effective exhaust velocity and specific impulse

η_{v*} = Correction factor for characteristic velocity

η_w = Correction factor for mass flow rate

 = friction loss coefficient

σ = Stefan Boltzmann Constant, 0.1714 x 10^-8 Btu/hr-ft^2-R^4

σ_c = Correction Factor

θ = Combustion chamber contraction angle

μ = Viscosity, lb/ft-s, Chemical potential, J/mol

1.0 INTRODUCTION

As we now look to the future of human exploration, Mars should clearly be the objective. It is the planet is most similar to the Earth, it has a 24 hour 37 minute day, and it contains the minerals that support life. It has been proven with robotic spacecraft and rovers that we already possess the fundamental technology to send humans to the planet, and that the technological breakthrough will simply come in developing and testing the hardware. This hardware will likely consist of a pressure-fed rocket propulsion system for both descent and ascent to and from the Martian surface. Therefore, it is our intent to design, manufacture, and test a pressure-fed rocket propulsion system.

2.0 LITERATURE REVIEW

2.1 Background and Context

When the late John F. Kennedy set our country the seemingly impossible goal of reaching the Moon within the decade, the United States had experienced a mere 15 minutes of human space flight, and yet, through the programs of Mercury, Gemini, and Apollo, we were able to reach that goal with 6 months to spare. One of the most vital pieces of these programs was the design and development of high-thrust rocket propulsion, a technology brought to the United States largely by former German physicist and rocket scientist Wernher von Braun. In 1961, rocket propulsion was still in its infancy, and was used almost entirely in high-thrust atmospheric applications. In order to lift the heavy mass required for a lunar landing into Earth orbit, the energy requirements dictated that NASA design and build a very large and very powerful first-stage engine, known as

the F-1, which powered the super heavy lift Saturn V rocket during the first phase of the lunar missions (see Figure 1).
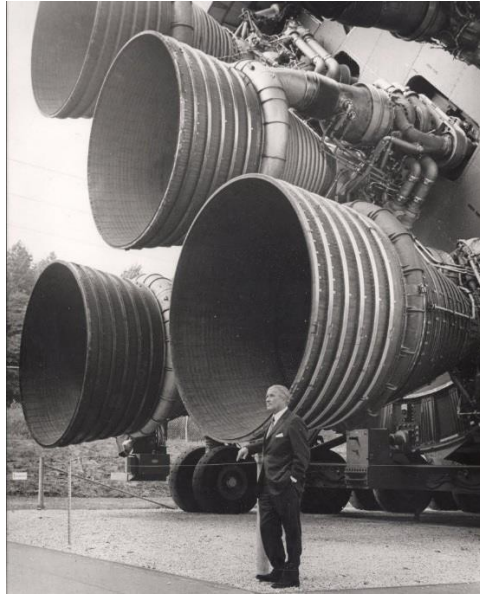
Figure 1: Wernher von Braun and the Five F-1 Engines of the Saturn V

These engines used what is known as a "Gas Generator Cycle", in which a small portion of the fuel was burned and converted into hot gas in order to power a turbine, which subsequently powered a turbopump that injected more propellant into the combustion chambers, and therefore, produce more thrust. This greater level of thrust was needed to escape the relatively high gravity well of Earth and insert its payload in to orbit. However, the plumbing system for this cycle can be complicated and expensive, which decreases reliability (see Figure 2).
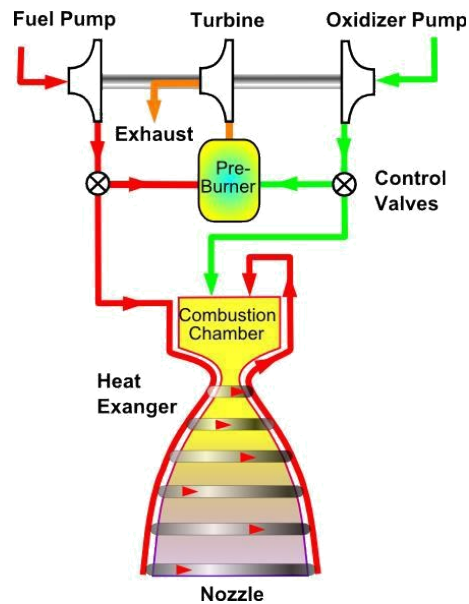
Figure 2: Schematic of a Gas Generator Rocket Engine Cycle

Additionally, once orbital velocity was achieved, the much lighter spacecraft no longer
needed these large amounts of energy from their propulsion systems. However, because
the spacecraft were going to be piloted, the propulsion systems, which were intended for
all ascent, descent, and course correction burns, needed to be both safer and more reliable
than their aspheric counter parts. Any anomaly within a propulsion system could have
meant catastrophic results for both the mission and the crew. With the principals of safety
and reliability in mind, the Apollo Service Module and Lunar Modules both utilized a
pressure fed rocket engines (see Figures 3 and 4). To improve reliability, the engines
utilized Aerozine 50 fuel, a 50-50 mass mixture of hydrazine and unsymmetrical
dimethylhydrazine (UMMD), and dinitrogen tetroxide oxidizer (N_2O_4).
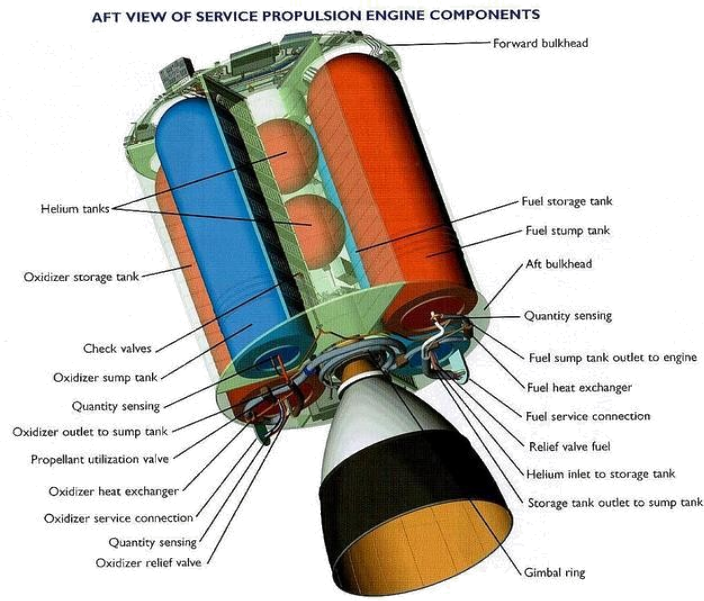
Figure 3: Apollo Service Propulsion System
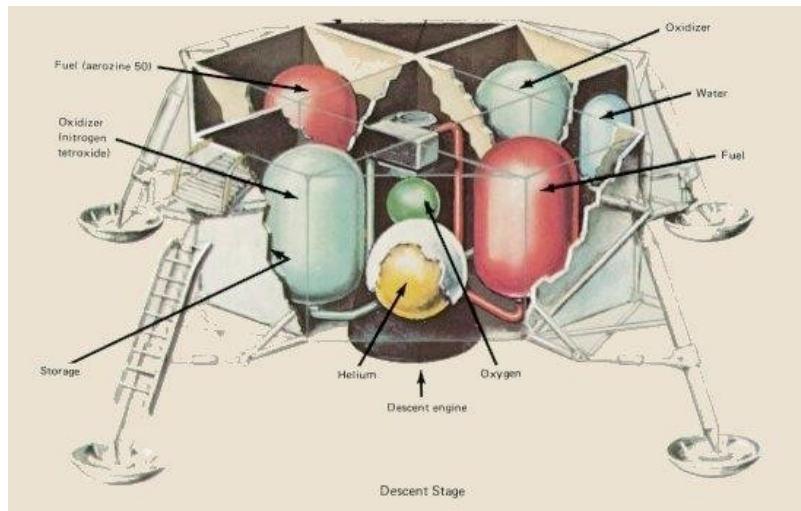
Figure 4: Apollo Lunar Module Descent Propulsion System

More recently, a new robotic rover weighing one metric ton, aptly named "Curiosity", landed on the Martian surface just 3 years ago. Given its large mass in comparison with that of previous rovers, a new landing technique was needed, called "Skycrane", where the descent stage used its own propulsion system to come to a complete hover over the landing site, lower the rover to the surface with 3 nylon tethers, and fly to a safe distance where it could impact the surface out of

the rover's path. This meant that the ability for the descent stage to decelerate to a stable hover was vital, and otherwise would have made the mission impossible. Therefore, similar to the Apollo program, the 8 Mars Landing Engines (MLEs) that provided to the impulse required to hover also utilized a pressure fed system, as well as hypergolic propellant, monopropellant hydrazine (see Figure 5). These propellant combinations were chosen specifically because of their hypergolic nature, in that the fuel ignited on contact either with the oxidizer, or in the case of monopropellant hydrazine, it loses electrons (or "oxidizes") independently. This meant a highly reliable system that did not rely on an ignition source.
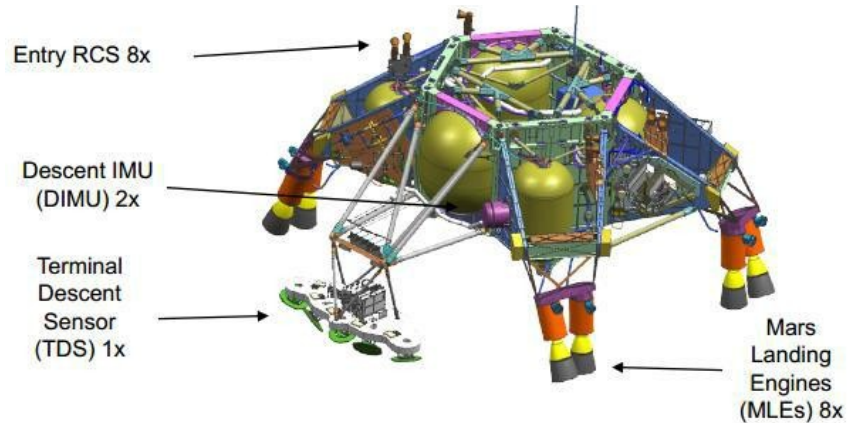
Figure 5: Mars Science Laboratory Descent Stage

2.2 Rocket Propulsion System Principles

The mechanics of a rocket engine are derived from the principle that an increase in gas temperature is proportional to its kinetic energy, its energy derived from motion. To express in elementary terms, hot gases move quickly (see Eq. 1).

$$= \frac{1}{2}{}^2 = \frac{3}{2} \qquad \text{(Eq. 1)}$$

Where:

KE = Kinetic Energy
m = Mass of the gas particle
v = Velocity of the gas particle
k = Boltzmann constant, equal to $1.38066*10^{-23}$
J/K T = Temperature of the gas particle

To achieve this increase in temperature, a combination of fuel and oxidizer are injected from their propellant tanks at an optimum mixture ratio, ignited, and reacted within the combustion chamber. As this chemical reaction builds up both temperature and pressure, the shape of the engine will force these hot gases into first a convergent section, where they accelerate to a sonic velocity (Mach 1). After reaching Mach 1 at the engine throat, these gases then travel through a divergent section, the nozzle, where they accelerate to supersonic speeds, expand, and lose heat. By the time the exhaust gases reach the exit of the engine nozzle, they will be traveling at their highest relative velocity, but also their lowest temperature and lowest pressure along the system (see Figure 6). The magnitude of increased velocity is dictated by the expansion ratio of the nozzle, the ratio of nozzle exit area to throat area. Additionally, the thrust of a rocket engine is dictated by the mass flow rate of the propellant, exhaust velocity, and pressure differential between the nozzle exit and atmosphere in which the engine is operating (see Eq. 2).

$$= \dot{}\ + (\ -\ \ \ \ \ )\ \ \ \ \ \ \ \ \ \ \ \ (Eq.\ 2)$$

Where:

F = Thrust
$= Mass flow rate$ = Exhaust velocity
= Nozzle exit pressure
= Atmospheric pressure
= Nozzle exit area
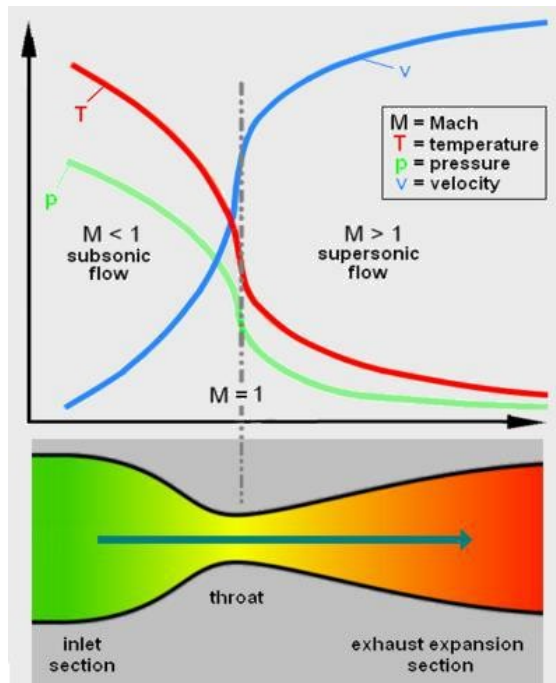
Figure 6: Gas Temperature, Pressure, and Velocity Profiles throughout a Rocket Engine

3.0 PRELIMINARY DESIGN AND APPROACH

A pressure-fed system is relatively simple. Rather than use a turbine as in the aforementioned gas generator system, a pressure-fed system utilizes a separate gas, usually helium, to pressurize the propellant tanks, forcing their contents through the injection lines and into the combustion chamber. Control valves situated on these injections lines will dictate the mixture ratio (see Figure 7).
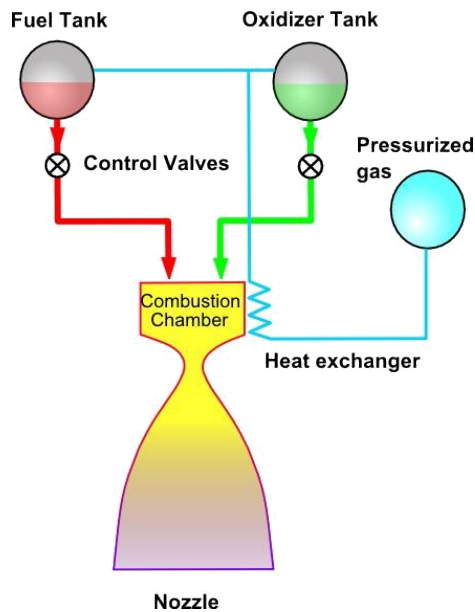
Figure 7: Schematic of a Pressure-Fed Rocket Engine System

3.1 Hypergolic vs Cryogenic

While previous descent and ascent rockets have used this rocket cycle, there are a considerable amount of disadvantages to using their propellant combinations. As previously mentioned, hypergolic propellants ignite on contact, and therefore do not require an ignition source, improving reliability. However, hypergolic propellants such as hydrazine, UDMH, and dinitrogen tetroxide, have a low specific energy, in that the amount of energy stored within a given mass is relatively low in comparison to other propellants. Additionally, hypergolic propellants are very toxic, carcinogenic, and corrosive. Because of this, extreme and expensive safety precautions must be undertaken during their use. Their effects were so severe that the Apollo engines used on the piloted vehicles could not be ignited until their actual use in space. For these reasons, one can conclude that hypergolic propellants would be both impractical and infeasible for this application.

3.2 The Case for Liquid Methane

The specific energy of any chemical compound is defined as the energy stored per unit mass. This is a key figure of merit due to the importance of weight restrictions in achieving orbital velocity. A CH_4/O_2 propellant contains almost 3 times as much energy per unit mass than hypergolic fuels used in other descent/ascent propulsion systems (see Figure 8).
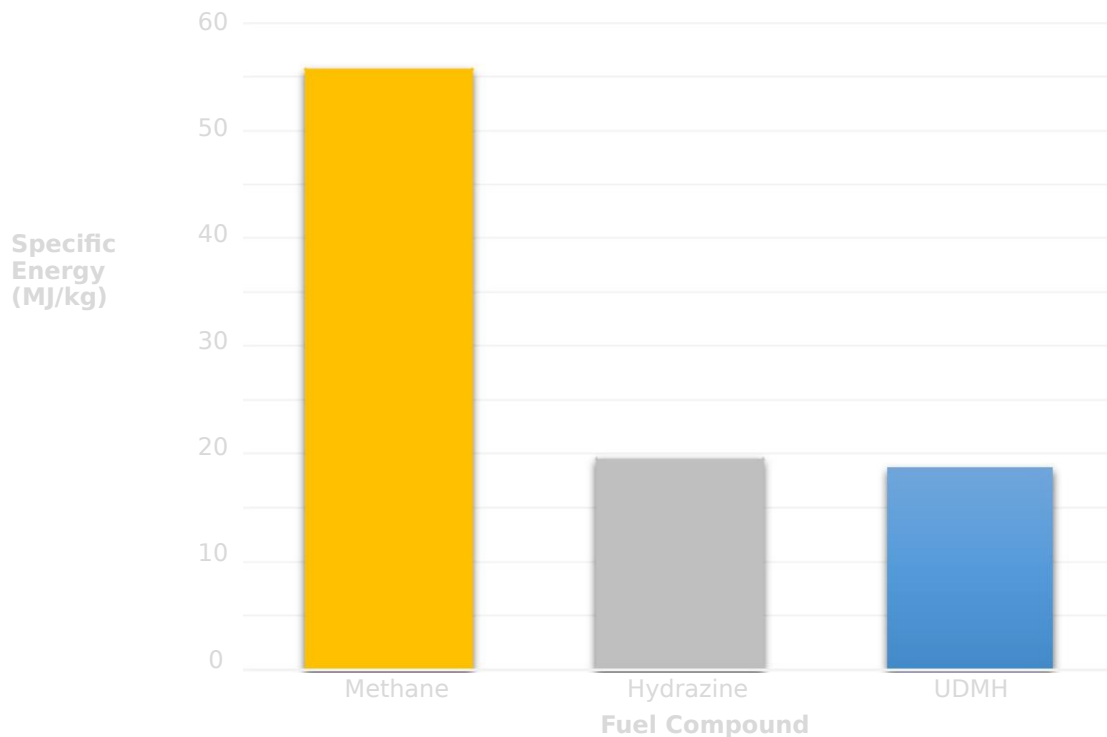
Figure 8: Specific Energy for Methane vs Hypergolics

Another method of decreasing launch mass requirements is the use of In-Situ Resource Utilization (ISRU), or more specifically, In-Situ Propellant Production (ISPP). Because carbon dioxide (CO_2) constitutes 96% of the Martian atmosphere, the most practical and useful combination is that which uses both carbon and oxygen, such as liquid methane (CH_4) and liquid oxygen (O_2). When combined with a feedstock of hydrogen, which only accounts for about 7%

of the mass of the CH_4/O_2 mixture, the propellant for a piloted ascent from the Martian surface can be manufactured by the very vehicle itself, negating the need to lift this mass from Earth and subsequently land it on Mars.

3.3 Analysis of Previous Applications

To date, there have only been four CH_4/O_2 rocket engines in development (see Table 1). However, the Raptor engine has yet to be tested and does not utilize a pressure-fed system, and the only 3D printed engine has extremely low performance. With this in mind, we aim to develop the first high performance 3D printed LOX/Methane engine. In order to make approximations for the design of our pressure-fed system, it is important to first analyze data from previous operational engines utilizing this cycle (see Table 2).

Table 1: Operational LOX/Methane Engines

Engine Name	Company	Engine Cycle	Thrust (N)	Manufacturing
Raptor	SpaceX	Staged Combustion	6,900,000	Machined/CNC
XR-5M15	XCOR	Pressure Fed	33,000	Machined/CNC
CHASE-10	DARMA	Gas Generator	98,000	Machined/CNC
Stiletto A1M	Masten	Pressure Fed	45	3D Printed

Table 2: Previously Operational Pressure-Fed Engine Data

Vehicle	Apollo DPS	Apollo APS	Kestrel	MSL MLEs
Total Landing/Liftoff Mass (kg)	15,000	5,000	10,000*	2,401
Propellant	Aerozine 50 (F) N_2O_4 (O)	Aerozine 50 (F) N_2O_4 (O)	RP-1 (F) O_2 (O)	Hydrazine (Mono)
Propellant Mass (kg)	8,200	2,353	3,800	390
No. of Engines	1	1	1	8
Chamber Pressure (kPa)	719	250*	930	200*
Min Thrust (N)	4,504	16,000	31,000	400
Max Thrust (N)	45,040	16,000	31,000	3,060
Max Total Thrust (N)	45,040	16,000	31,000	24,480
Vacuum Isp (s)	311	311	317	221
Max Mass Flow Rate (kg/s)	14.8	5.2	10.0	11.3
Minimum Burn Time (s)	555	448	381	34
Thrust-to Weight	25.7	19.9	65.0	30.0*

*Approximate

Design work was performed using various programs. Preliminary calculations and simulations were performed using Microsoft Excel, Rocket Propulsion Analysis (RPA) and NASA's Chemical Equilibrium with Applications (CEA) program. Additional code for a thermodynamic analysis was created in order to provide a check for the various thermodynamic properties. Computational Fluid Dynamics were performed using programs such as ESI and Star CCM+. Finally, all computer models were created using AutoCAD and SolidWorks.

3.4 Manufacturing and Testing

Similar to most propulsion systems, a majority of our propulsion system will be comprised of aluminum alloys and stainless steel. GPI Prototype and Manufacturing in Oak Bluff, IL will be used to 3D print the engine, given their experience with previous rocket engines of similar caliber. The material used will be Cobalt Chromium, a relatively strong material, both structurally and thermally, and has proven to work well with other static tests.

Some of the funding will be raised in-house, while sponsorship through SEDS, AIAA and/or other aerospace companies will most likely be required for additional funding and fabrication.

If a test stand cannot be fabricated, there are various testing facilities in the western United States, including California, Washington, Utah, New Mexico, and Texas. We have also been in contact with UCSD to use a test stand that they have built and previously used to test rocket engines of a similar scale.

3.5 Scheduling

Table 3: Gantt Chart

	Month	Stages	
FALL SEMESTER	September	Literature Review	Preliminary Design
	October	Funding Research	Critical Design
	November		
	December		Computer Simulations

SPRING SEMESTER	January	Fabrication	Funding
	February		
	March		
	April		Systems Integration
			Testing
	May		Report Writing/ Presentation Planning
			Presentation

3.6 Design Methodology and Approach

The following design methodology was chosen and was used throughout the duration of the project. (see Figure 9). The team did not look into vehicle selection, as this project only focuses on the propulsion system of the vehicle.
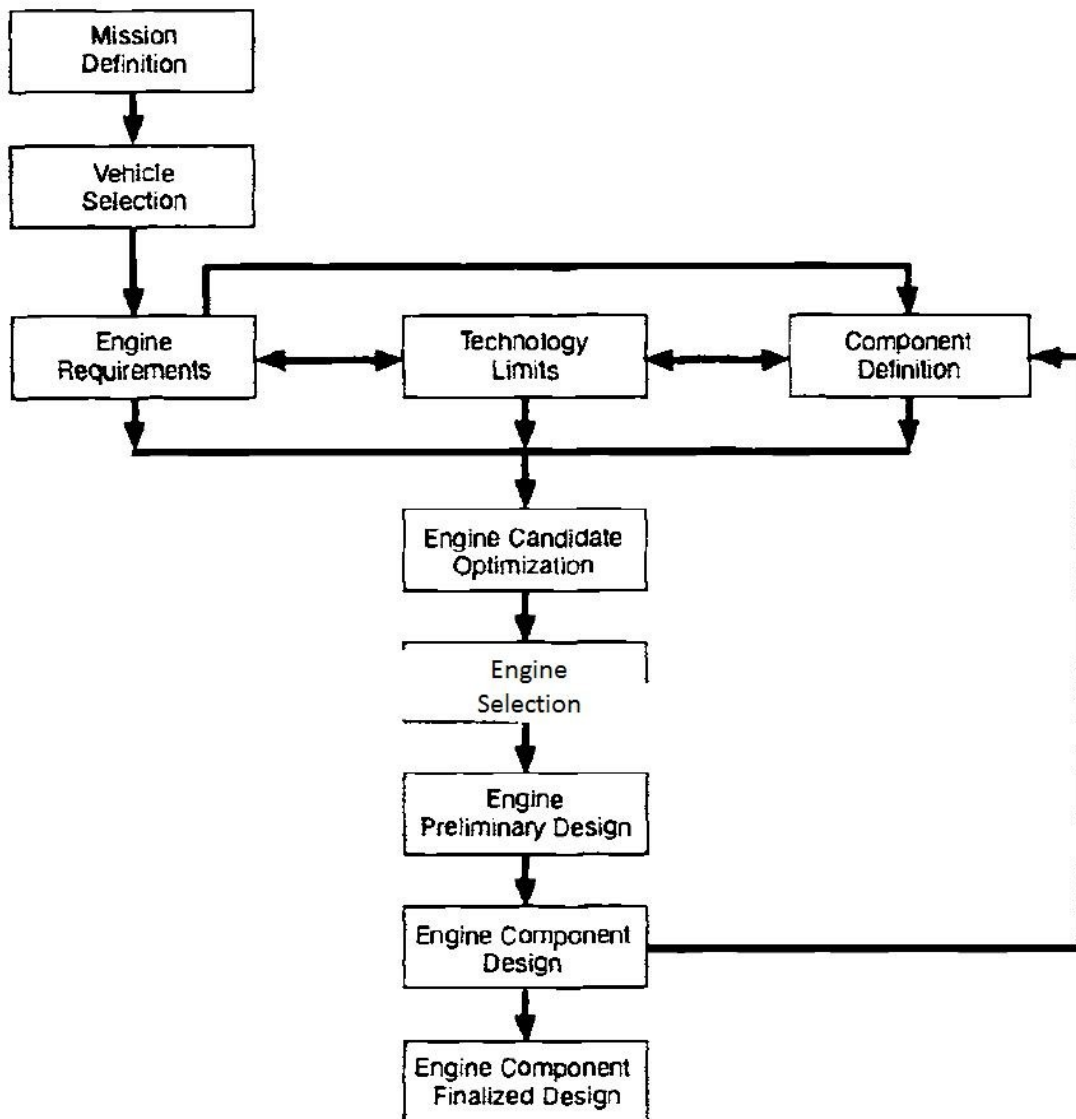
Figure 9: Flowchart for Rocket Engine Preliminary Design

4.0 CONCEPTUAL DESIGN

4.1 Mission Definition

To design, print, and test a LO$_2$/LCH$_4$ rocket engine to further develop the technology required to land humans on Mars.

4.2 Mission and Design Requirements (Success Criteria)

The following Mission and Design Requirements were provided by Friends of Amateur Rocketry in order to successfully test our engine at their predesignated location. This procedure is outlined in further detail in Appendix A.

Testing Requirements:

- Tank Hydrostatic Test
- Water Flow Test
- Injector Water Flow Test
- Rocket Valve Test
- Leak Test
- Rocket Static Test

Design Review Requirements:

- Rocket Design Review Checklist
- Rocket Static Firing Design Review Checklist
- Ground Support Equipment Design Review Checklist

4.3 Mission and Design Parameters

4.3.1   Thrust

The thrust decision can often be made by observing previous engines in production for a specific mission in order to reduce costs in research and development. As previously mentioned, it has already been determined that this engine will be unique in its combination of manufacturing, engine cycle, and propellant combination. Our designs were initiated by designing for ideal expansion, ie: setting the exit pressure to the ambient pressure in order to obtain nominal thrust during our sea level static test.

4.3.2   Performance

The performance of the thrust chamber is a direct function of the parameters listed in Table 3. Of these parameters performance is mainly measured on specific impulse therefor changing these parameters around as much as possible within our design limits in order to increase specific impulse (I_{sp}). The characteristic velocity (c*) is used to rate the propellant combustion performance and the thrust coefficient is a dimensionless parameter that is used to measure the gas expansion through the nozzle.

Table 4: Ranges of Performance Parameters of Liquid Rocket Engines

Performance Parameters	Symbol	Units	Range
Gas temperature	T	°R	4000-7000
Nozzle stagnation temperature or chamber total pressure	$P_{c_{ns}}$	psia	10 - 2500
Molecular weight	$\dot{m}$	g/mol	2- 30
Gas constant	R	in-lb/slug °R	51.5- 772
Gas flow Mach number	M		0-4.5
Specific heat ratio	γ		1.13-1.66
Nozzle expansion area ratio	□		3.5-100
Nozzle contraction area ratio	$□_c$		1.3-6.0
Thrust coefficient	C_f		1.3-2.0
Characteristic velocity	c*	ft/s	3000-8000
Effective exhaust velocity	c	ft/s	4000-12000
Specific impulse	I_s	s	150-480
Correction factor for thrust and the thrust coefficient	$η_f$		0.92-1.00
Correction factor for effective exhaust velocity and specific impulse	$η_v$		0.85-0.98
Correction factor for characteristic velocity	$η_{v*}$		0.87-1.03
Correction factor for mass flow rate	$η_w$		0.98-1.15

4.3.3   Burn Duration

Previously tested rocket engines lie within a burn duration of 50-500 seconds based on their corresponding mission requirements. Choosing an appropriate burn duration is vital due to its dependence on the required initial mass of the system, including payload, structural mass, tank capacities, pressurization tank supply, and uncooled temperatures for engine/nozzles. The quality of the propulsion system is further measured by compliance with specified thrust over this burn duration, maximum rate of increase during build up, freedom

from surges or overshoots, smoothness, and repeatability. For this application, designs utilized a relatively low burn duration to simply prove the functionality of an engine during a test.

4.3.4 Mixture Ratio

The mixture ratio is defined as the ratio of mass flow rate of the oxidizer to that of the fuel. The stoichiometric ratio of a propellant combination, the ratio at which the fuel will be completely oxidized, is typically higher than that of the actual mixture ratio used in the propulsion system of a rocket. This is primarily due to two factors. First, mass optimization of a launch vehicle is crucial, particularly when being launched within a strong gravity well. Since the oxidizer is almost always more dense than the fuel, the system will utilize a larger amount of fuel, and therefore, a lower mixture ratio. Additionally, fuel is typically used as coolant within the chamber and nozzle, so more fuel is usually required to facilitate this design. Sacrifices in mixture ratio will therefore correlate to sacrifices in engine performance but allow gains in other areas such as weight, chamber wall cooling, and smaller tank sizes.

4.3.5 Weight

Success of a rocket engine is most commonly defined as weight or mass of payload per dollar spent, meaning that the design weight of the overall system is a critical factor for commercial customers as well as making a valuable investment. Additionally, the final velocity of the launch vehicle is a function of the launch mass ratio, which is involves the mass of the propellant. Typically, propellant constitutes about 89% of the total mass of a launch vehicle or rocket stage utilizing a pressure fed propulsion system, however, our engine design will not be integrated into a launch vehicle.

4.3.6 Envelope size

The envelope size is the geometric design constraint that defines the volume of the combustion chamber as well as the overall dimensions of the engine. This size will factor into the structure, weight, handling equipment, cost, manufacturing machinery availability, storage, and transportation of the launch vehicle. For our application, we are choosing to 3D print the entire assembly in order to streamline manufacturing and ensure mass production of a LOX/LCH4 propulsion system.

4.3.7 Reliability

Reliability is extremely critical to a propulsion system due to the high cost of launching payloads to orbit, or in the case of human space flight, the prospect of human fatalities. Since the long term application of this type of propulsion system is to be used on a piloted Martian lander and/or ascent vehicle, reliability would be crucial to the success of the mission. In addition to reaching or exceeding our performance figures, our goal is to ensure a smooth, efficient combustion process while also possibly reusing the engine at a later date after the initial test.

4.3.8 Cost

When formulating a budget for such a low-cost project, it is imperative to refrain from certain initial design mistakes. These mistakes include the reliance on outsourcing facilities, supply of materials, and propellants that may not be available in the foreseeable future. It is also important to make the design relatively simple, to keep manufacturing both rapid and cost effective, while preferably designing the system to be reusable.

From the analysis above we aim to reach the following parameters

- **Propellant:** Liquid Oxygen and Liquid Methane
- **Chamber Pressure:** 1,040 psi (7.2 MPa)
- **Thrust:** 2,050 lbf (9,000 N)
- **Isp:** 300 seconds (Sea Level)
- **Duration or Burn time:** 10 seconds
- **Envelope Size:** 9.85 in x 9.85 in x 12.8 in

4.4 Applied Mission Goals

The following mission goals were decided based upon the mission requirements and parameters mentioned above with the corresponding point's breakdown to allow for mission success.

- Simplicity (5)
- Envelope Size (4)
- Performance or Isp (3)
- Low cost (2)

4.4.1 Simplicity

Simplicity is the most important goal for the project because this is the first time a rocket propulsion group at San Jose State University will attempt such an endeavor. We aim to greatly simplify manufacturing of the entire rocket propulsion system by only manufacturing all individual components, including the injector, chamber, and nozzle, into one single piece. This is possible due to the recent development and advancement of Direct Metal Laser Sintering (DMLS), which takes a bed of powder and sinters the material on a 2-Dimensional plane moving vertically, thus creating a 3-Dimenstional object.

23

Simplicity not only in the sense of DMLS manufacturing but also in advanced techniques in order to achieve our goal. The project is designed as a first year project with the intent to continue annually to educate continuing students in rocket propulsion.

4.4.2 Envelope Size

Envelope Size is defined as the maximum volumetric constraint given by the machine that is most cost effect to use for DMLS manufacturing. The machine will be provided by GPI Prototype and Manufacturing, which has had experience in printing a single rocket engine with different propellant combinations. The machine in use by GPI is the EOS M280, which has an envelope size of 9.85in x 9.85in x 12.8in in the x, y, and z axes respectively. The EOS M280 has an accuracy of 0.02mm (7.87×10^{-4}in), a minimum internal structure diameter of 0.8mm (3.14×10^{-2}in), and a minimum under-sizing thickness of the drill holes of 0.6mm (2.36×10^{-2}in) in order to re-bore the cooling channel. The surface roughness of the EOS M280 is provided as 8.75 Ra-μm (350 Ra-μin) before any post processing.

4.4.3 Performance

Performance is simply, the highest achievable specific impulse or I_{sp} without tradeoffs to simplicity and envelope size as those goals hold a higher weight for mission success.

4.4.4   Cost

Low Cost is also a function of the EOS M280 as cost increases with material used, total height of the part, and hours the machine is running. Low cost is also the driving factor for the majority of the non-printed parts such as the propellant feed system.

4.5 Team Development and Subsystem Overview

A portion of the design process involved the initiation of a chapter of an international organization, Students for the Exploration and Development of Space (SEDS). Since its inception during the Spring semester, this project has become the primary project for SEDS at SJSU.

Our team is broken down into five separate subsystems that contain overlapping part designs. Therefore, we took a systems engineering approach and defined each system based on a component analysis rather than a discipline system analysis
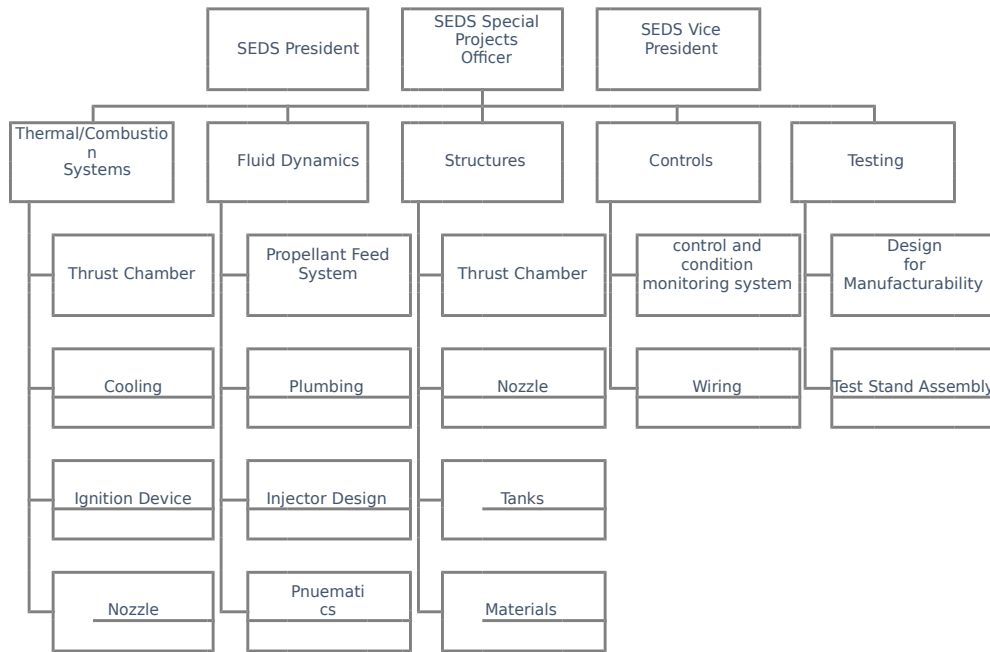
Figure 10: Flowchart for Rocket Engine preliminary Design

4.6 Component Configuration Selection

In order to efficiently streamline the design of our propulsion system we looked into each subsystem component and rated each option in order to begin the preliminary design. Each component incorporated at least three options in order to decide on the optimal component for our specific mission. The selection process was conducted for the combustion chamber, nozzle, cooling system, injector system, ignition device, and propellant feed system based on the weighted mission goals previously provided. From here, each component was weighted on a scale of 1 to 5 based on its effectiveness, or importance, on the overall system. For example, the thrust chamber affects the performance at a magnitude far greater than that of the igniter device. Therefore, the chamber was given a component weight of 5 for performance, while the igniter device is only given a 1. The weighted mission goal is then multiplied by the weighted

26

component goal, before being multiplied by the configuration weight and then added to the total sum. The configuration with the largest sum total is the obvious choice for our designs.

4.6.1 Combustion Chamber

Table 5: Combustion Chamber Decision Matrix
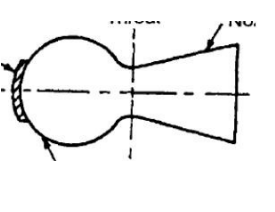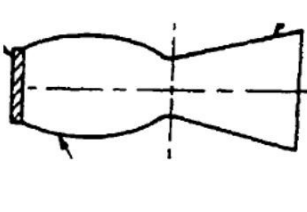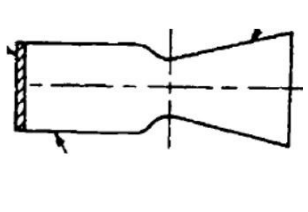
Combustion Chamber		Spherical	Near Spherical	Cylindrical
Mission Goals	**Component**	**Spherical**	**Near Spherical**	**Cylindrical**
Simplicity 5	5	1	3	4
Envelope Size 4	5	5	4	3
Specific Impulse 3	5	5	4	3
Cost 2	3	4	3	1
Totals:		224	233	211

Historically, there are three main chamber shapes that have been utilized for liquid rocket engines: spherical, near-spherical, and cylindrical, each having its own advantages, including weight, cooling, stability, and ease of manufacturing. For example, spherical and near-spherical combustion chambers require a lower surface area and therefore require less cooling and less mass due to its pressure characteristics, but their geometric shape is relatively difficult and more expensive to manufacture traditionally.

Due to recent advances of direct metal laser sintering (DMLS), the spherical and near spherical options have become once again feasible and simple. The near spherical combustion

27

chamber was chosen due to its major gains in structural performance and overall length, with minimal losses in simplicity.

4.6.2   Nozzle

Table 6: Nozzle Decision Matrix
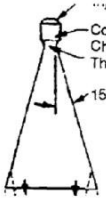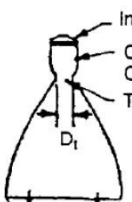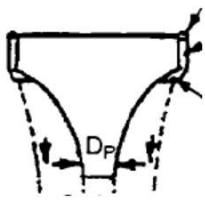
Nozzle			Conical	Bell	Aerospike
Mission Goals		**Component**	**Conical**	**Bell**	**Aerospike**
Simplicity	5	1	5	4	1
Envelope Size	4	5	1	5	1
Specific Impulse	3	4	4	3	5
Cost	2	5	3	4	1
Totals:			123	196	95

In order to achieve a higher performance with a lower weight, the bell nozzle, which involves a parabolic contour as opposed to a linear geometry, was chosen for the final design. The gradual contour in this design considerably decreases the chance of an oblique shock, which may occur with an instantaneous change in direction of supersonic flow. The design of this geometry is based off the half angle of a conical nozzle, the most common of which is 15 degrees. The nozzle is then designed using a fractional length of the conical nozzle, L_f, the most common of which is 80%. The design not only reduces weight but reduces the volume of the nozzle, which is shown in the envelope size breakdown above. Similar to the utilization of a near spherical combustion chamber, the bell nozzle also lowers costs due to lower amount of required material, the main driving factor in DMLS manufacturing.

4.6.3 Cooling System

Table 7: Cooling Configuration Decision Matrix
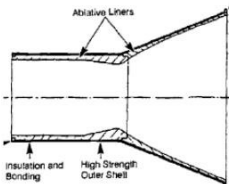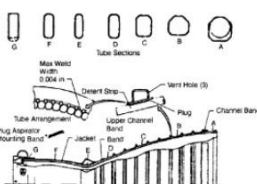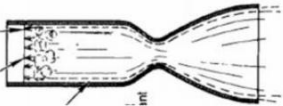
Cooling			Ablative	Regenerative	Film
Mission Goals		**Component**	**Ablative**	**Regenerative**	**Film**
Simplicity	5	5	3	4	5
Envelope Size	4	1	5	5	5
Specific Impulse	3	5	5	5	3
Cost	2	1	3	4	5
Totals:			176	203	200

Regenerative cooling is the most widely used method of cooling in engineering practice. This method consists of at least one of the propellant elements, usually the fuel, being fed through a series of channels within the chamber walls that absorb a portion of the heat applied to the engine material. In ablative cooling, heat is dissipated by sacrificing a small amount of the interior chamber wall. During combustion, the melting and vaporization of this "ablative liner" will effectively minimize the amount of heat transmitted to the high strength outer wall of the engine. This technique is typically used in solid rocket engines or liquid rocket engines with low combustion pressures. Film cooling occurs by orienting several orifices around the injector plate that will direct a portion of the propellant directly to the chamber walls. This "film" of cooler liquid essentially protects the inside of the chamber walls from the heat of combustion, which is generally concentrated toward the center.

Traditionally, ablative cooling is known to be easier to manufacture than regenerative cooling. However, as shown above, regenerative cooling was chosen for its performance and 29

relative simplicity. Additionally, DMLS manufacturing makes it is impossible to apply a separate, ablative layer in the combustion chamber, so it generally more feasible to create internal cooling walls for regenerative cooling. There are performance losses in specific impulse with film cooling, but due to the thermal properties of cobalt chromium, this was determined to be the necessary method of cooling.

4.6.4   Injector

Table 8: Injector Configuration Decision Matrix
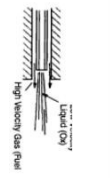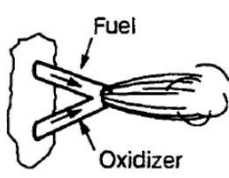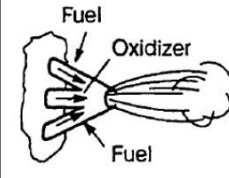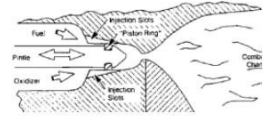
Injector Configuration					
Mission Goals	Component	Coaxial	Unlike Doublet	Unlike Triplet	Pintle
Simplicity	5	5	3	5	5	1
Envelope Size	4	2	2	3	3	2
Specific Impulse	3	5	3	3	4	5
Cost	2	3	3	3	3	2
Totals:		154	212	227	128

The injector design will be absolutely critical, as it has the largest impact on the combustion performance. This piece of the engine has multiple functions, but its main purpose is to properly inject and mix the propellant elements to ensure both stability and efficiency of the combustion process. It is also important that a proper pressure drop occur across the injector plate, usually about 20%, due to the possibility of combustion fluctuations that may lead to combustion

30

instability. Injection of the propellants can occur in multiple different fashions, each of which has different advantages and disadvantages of stability and performance (see Table 8). A number of different configurations for each element type were also considered.

Table 9: Performance Characteristics for Various Injection Plate Orifice Elements

Element Type	Combustion Stability Level	Performance Level
Non Impinging	High	Low
Like-Impinging	Moderate	Moderate
Unlike-Impinging	Low	High

Coaxial injection is the most common injection configuration for non-impinging propellant streams. This type of injector typically incorporates a slow-moving center stream of liquid oxidizer surrounded by a sheet of gaseous fuel at very high velocities. Coaxial injection is well-suited for propellants using a gaseous fuel, as it is difficult to achieve the velocity deferential between the two elements required to create the desired performance.

A pintle injector is a form of a coaxial injector. First used in the Apollo Lunar Module Descent Engine (LMDE), a pintle injector first involves injecting the fuel through an orifice in the nozzle body and into a chamber above a needle valve. As the pressure builds in this chamber, the force of this fuel pressure acts on the tapered edges of the valve until it overcomes the force of a spring upstream of the injection orifice. The areas of the orifices out which the fuel and oxidizer flow are therefore dependent on the amount of pressure pushing on the needle valve. This allows both fuel and oxidizer to be injected at predetermined flow rates based on mixture ratio. This configuration is especially useful in throttling engines, but is also more expensive and more difficult to manufacture.

Unlike doublet injection is the most basic form of mixing two propellant elements. These involve a stream of oxidizer and a stream of fuel injected at angles that will impinge on one another, producing a fan-shaped spray within the combustion chamber. This will subsequently create a resultant angle, $\square$, computed from the momentum of the two different streams. Unlike doublet streams offer high performance, but also are susceptible to combustion instability. Because the oxidizer mass flow rate is almost always larger than that of the fuel, "misimpingement" and imperfect mixing can occur, causing inefficient and irregular combustion that may lead to non-ideal performance and even damage to the engine.

Unlike triplet injection is the most basic form of mixing two propellant elements. These involve 2 streams of either fuel or oxidizer and 1 stream of the other, injected at angles that will impinge on one another, producing a fan-shaped spray within the combustion chamber (see Figure 31). Unlike triplet streams offer high performance as unlike doublets, and are less susceptible to combustion instability. Because the oxidizer has a larger mass flow rate compared to that of the fuel component, it will require more orifice area. However, when utilizing propellants at lower mixture ratios, an orientation of 2 oxidizer orifices and 1 fuel orifice allows the orifice sizes to be much more similar, creating a similar momentum and directing the propellant axially through the chamber. This type of injection also creates a better mixture between the propellants, leading to a smoother and more efficient combustion process.

4.6.5 Ignition Device System

Table 10: Ignition Device Decision Matrix
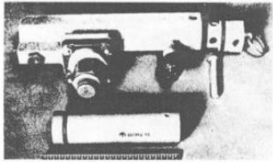
Ignition Device			Pyrotechnic	Hypergolic	Spark Plug
Mission Goals		**Component**	**Pyrotechnic**	**Hypergolic**	**Spark Plug**
Simplicity	5	5	5	1	4
Envelope Size	4	4	5	3	4
Specific Impulse	3	1	1	1	1
Cost	2	5	5	1	3
Totals:			258	86	197

In order to the release the chemical energy stored in the propellants, an ignition device must be used to initiate the combustion process. This igniter device will have one major function: rapid and reliable ignition of the propellants before an overwhelming amount of build-up of reactive material can occur. If the ignition process is not immediate, this build-up can have disastrously explosive effects. Various ignition devices and options were considered.

Pyrotechnic igniters utilize an electrical explosive that ignite a small amount of solid propellant. These are usually mounted either to the injector face or through the injector from the manifold side. It is important for the igniter to both ensure early ignition and enhance heat distribution, so a robust igniter will incorporate flame-spreading designs. These designs provide a "sheet" of flame downstream of the impinging elements, causing them to combust immediately after mixing.

Hypergolic ignition systems utilize hypergolic propellants, ie: a fuel and oxidizer that ignite on contact. This type of ignition typically uses a small amount of fluid hypergolic with the oxidizer that is stored in a cylindrical chamber with rupture discs at both ends. The rupture discs in the hypergolic cartridge fail at a predesigned pressure, and the hypergolic fluid impinges on the oxidizer stream in the chamber, igniting immediately. This ignition flame is then sustained by the subsequent flow of fuel. A common type of hypergolic ignition fluid is a mixture of triethylaluminium-triethylborane, also known as TEA-TAB. Hypergolic propellants are very reliable for combustion although are toxic, unstable, and expensive.

With spark plug ignition devices, somewhat similar to an internal combustion car engine, electrical current is sent from a capacitor to deliver multiple sparks per second. These sparks then ignite the propellants and initiate the combustion process. Spark plugs have become extremely reliable and are suited for engines requiring multiple ignition sequences without servicing in between. However, this ignition device may need additional manufacturing and may adversely affect the design of the injector, leading to higher costs.

Table 11: Propellant Feed System Decision Matrix

Propellant Feed System				
Mission Goals	**Component**	**Blow Down**	**Pressure Fed**	**Turbopump**
Simplicity	5	5	5	4	2
Envelope Size	4	1	1	1	1
Specific Impulse	3	4	1	4	5
Cost	2	3	5	4	1
Totals:			171	176	120
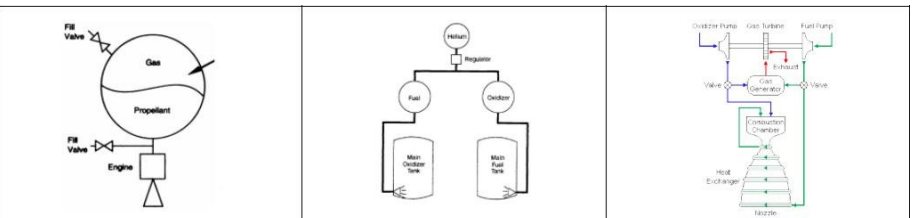
The method of propellant transfer from the tanks to the injector can have drastic effects on the performance of a propulsion system. In practice, propellant tanks are pressurized to a certain level, usually based on a combination between required flow rate and material strength. Different engine cycles offer different advantages and disadvantages based on cost, manufacturing, and performance requirements.

Pressure-fed injection systems use a gas, usually helium, to pressurize the propellant tanks to a pre-designated pressure for proper mass flow rate. A valve regulates the pressure within the tanks to maintain constant pressure and thrust from the engine.

Blow down feed systems utilize pressurized tanks, but unlike typical pressure-fed systems, they do not include a regulator on the pressure valve. This negates the need for a pressurizing gas but allows for undesirable variations in thrust.

If higher thrust is required, this in turn requires a higher flow rate. In turbopump feed systems, such as a gas-generator engine cycle, a small portion of fuel is usually combusted in a pre-burner, whose exhaust gas powers a turbine. The turbine then powers the turbopumps in order to inject the propellant at higher velocities. This method is preferable for very high thrust values, but is also more complicated and costly.

For reasons mentioned above the pressure fed system was chosen based on its gains in performance with hardly any losses in simplicity.

5.0 FINAL DESIGN

Before a design began, it was important to understand the principals of rocket propulsion. Fluid analysis and physics analyses were performed, followed by trade studies for each engine component.

Assumptions:

- Isenthalpic combustion in chamber
- Adiabatic, isentropic frictionless and no dissipative losses
- Quasi-one-dimensional nozzle flow for both shifting and frozen equilibrium models and in chamber and nozzles
- Ideal gas law
- No dissipative losses
- Conservation of mass, momentum, and energy throughout

5.1 Thermodynamic Fluid and Physics Analysis

Referring back to Eq. 2, we see that the engine thrust (or "momentum thrust") is a function of the mass flow rate and exhaust velocity, and the pressure thrust is a function of the forces due to the pressure differential at the nozzle exit. However, like in many engineering problems, there is a compromise. While the mass flow rate will remain constant through the entire system, the exhaust velocity will fluctuate with the expansion of the gases through the nozzle. For a given atmospheric pressure, the nozzle may be over-expanded, under-expanded, or ideally expanded. During over-expansion, the gases are accelerated to a very high velocity by the time they reach the nozzle exit, but the exit pressure will be also be considerably lower than the pressure and therefore subtracting from the pressure thrust created by the engine. Conversely, during under-expansion, the gases are not accelerated to an optimum velocity, but because the exit pressure is higher than that of the ambient atmosphere, the engine will gain pressure thrust. The ideal case is a middle ground, where the exit pressure and ambient pressure are equal, and the engine will rely solely on its exhaust velocity to produce its thrust. For a given altitude, and therefore a given atmospheric pressure, it is this ideal condition where thrust will be maximized (see Figure 10).
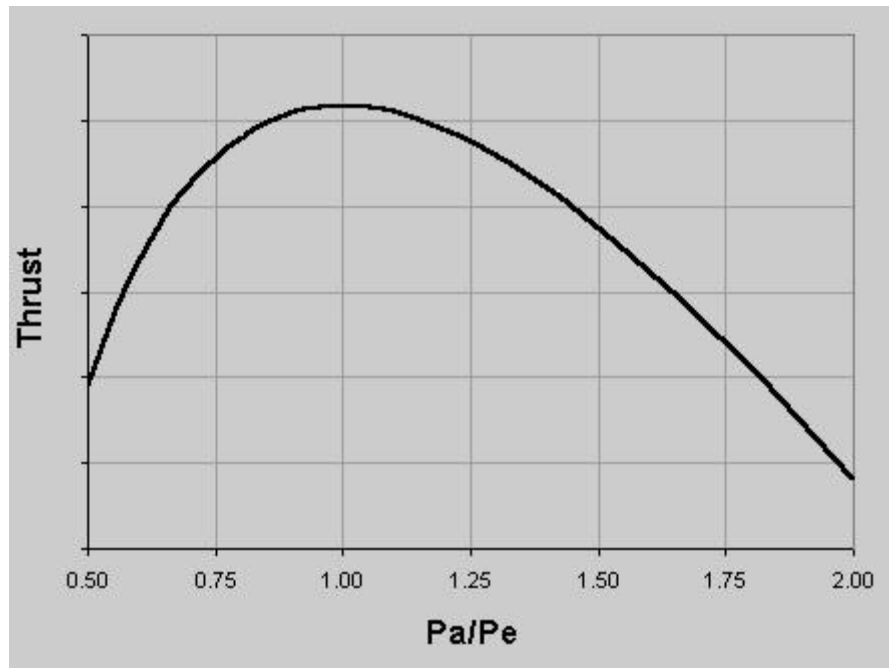
Figure 10: Thrust vs. Exit Pressure Ratio

Since we will be testing the engine at sea level, it will be advantageous to design the nozzle for ideal expansion ($P_a/P_e = 1$). This is validated by the fact that a landing craft will likely need its largest amount of thrust when it is within close proximately with the terrestrial surface, allowing it to achieve a soft landing.

When designing a rocket engine, we must first designate certain values as "input values" and others as "output variables". In this particular design case, the two most important input values will be mass flow rate ($\dot{m}$), combustion chamber pressure (P_c), and exit pressure (P_e). Because the gas inside the chamber will be largely stagnant, we can assume this value to be the "stagnation pressure" or "total pressure", which will hold true throughout the system as dictated by the principles of an isentropic process. Additionally, we will set our exit pressure to be equal to 1 atmosphere (101.325 kPa or 14.7 psi at sea level).

Since the pressure differential at the nozzle exit is nullified during ideal expansion, the exit velocity is therefore the most crucial variable in determining the magnitude of thrust. In turn, this value is dependent on a number of other properties of the gas itself (see Eq. 3).

$$v = \sqrt{\left(\frac{2}{\gamma - 1}\right)\left(\frac{\gamma R^* T}{M}\right)\left(1 - \left(\frac{p}{p}\right)^{\frac{\gamma - 1}{\gamma}}\right)} \tag{3}$$

Looking at this equation, it seen that there are 3 variables (ratio of specific heats, chamber temperature, and molecular mass) that are unknown at the outset of the analysis. These variables can be referenced for a given element, but are much more complicated to obtain for a propellant mixture. To find these values, we must first obtain the optimum mixture ratio for the given oxidizer and fuel, which we have chosen as liquid oxygen (LO$_2$) and liquid methane (LCH$_4$), respectively (see Figure 11).
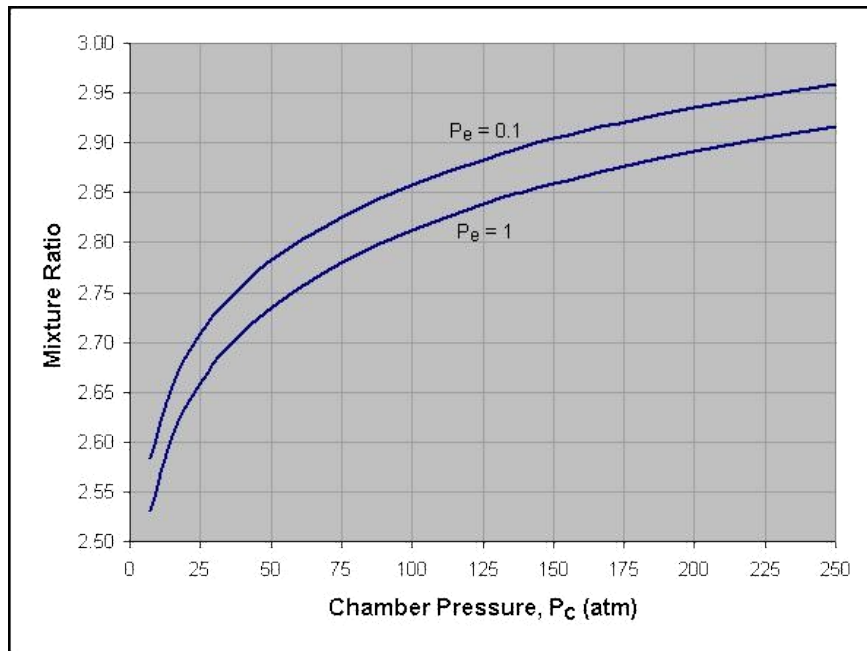
Figure 11: Mixture Ratio vs. Chamber Pressure for a given exit pressure

Because we found the need to experiment with the exact value for chamber pressure, it was vital to extract the data from the figure and formulate a polynomial algorithm so the optimum mixture ratio could be obtained much quicker. Once this equation was obtained, we could repeat the process for the remaining variables (see Figures 10, 11, and 12), before checking their accuracy with RPA in addition to our own calculations.
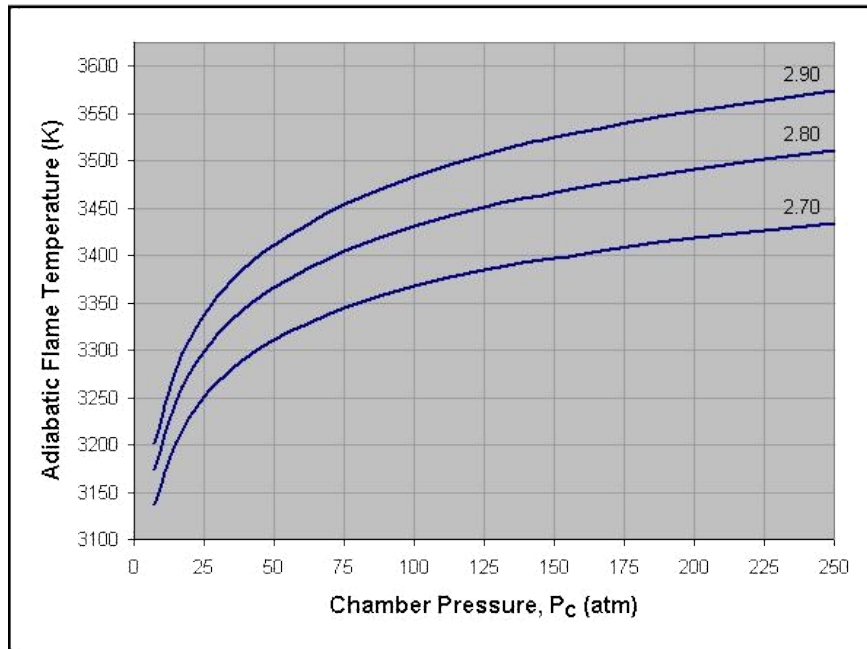
Figure 12: Adiabatic Flame Temperature vs. Chamber Pressure for a given mixture ratio
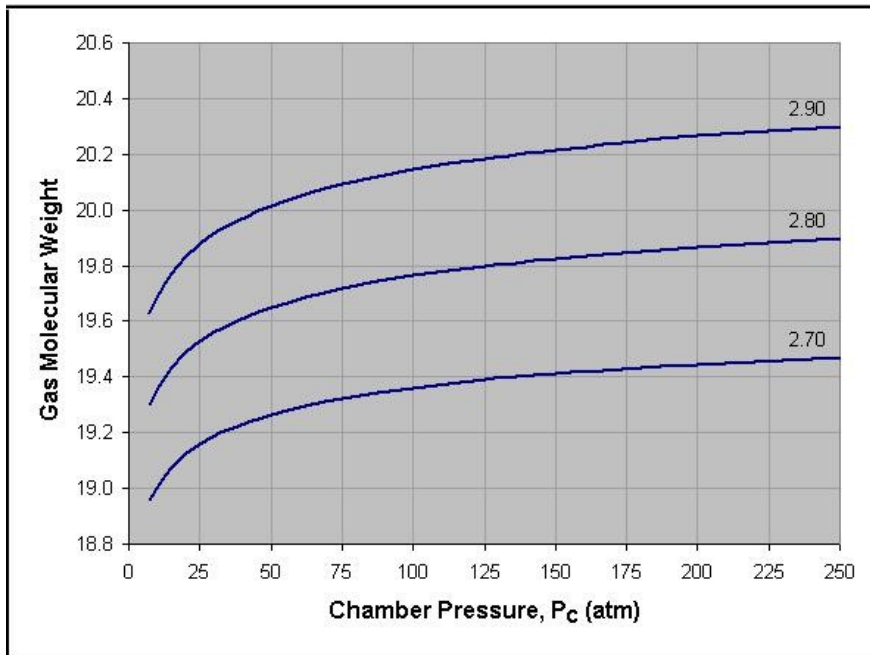
Figure 13: Gas Molecular Mass vs. Chamber Pressure for a given mixture ratio

41
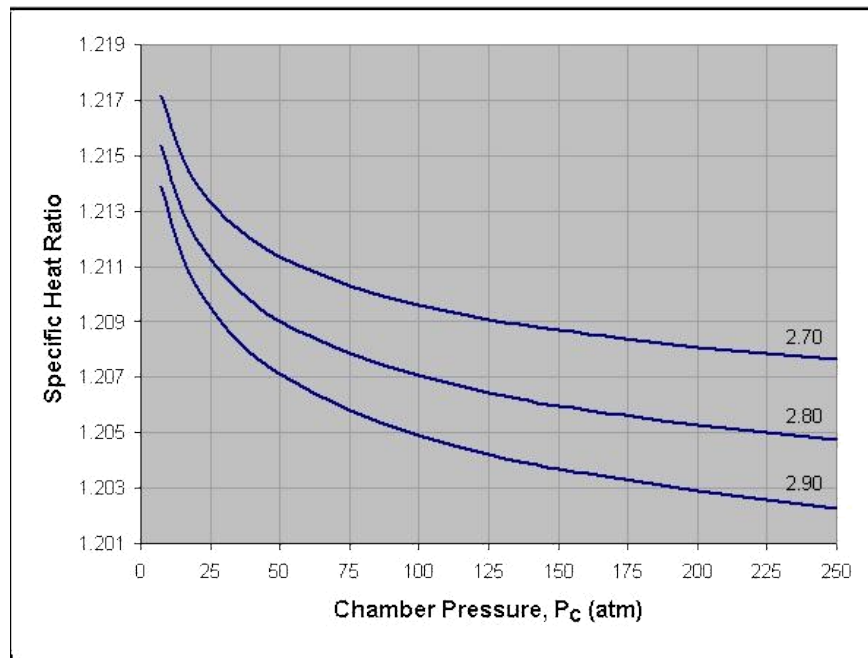
Figure 14: Specific Heat Ratio vs. Chamber Pressure for a given mixture ratio

5.1.1 *Thermodynamic Combustion Analysis*

As propellants are ignited in the combustion chamber at the constant injection pressure, energy stored within the chemical bonds in each compound is released in the form of heat. It was necessary to calculate this amount of heat, or enthalpy, in order to accurately back-calculate the combustion temperature, molecular mass, and ratio of specific heats.

The first law of thermodynamics dictates that energy remains constant through the entire system. Internal energy, U, is transferred in two different forms: heat, Q, and work, W (see Eq. 4).

$$= + \qquad\qquad (4)$$

Enthalpy, a state variable, takes into account the internal energy within the system as well as the work done by the gas to make room for the system, known as pressure-volume work (see Eq. 5).

$$= \ + \ = \ + \ + \tag{5}$$

Since total enthalpy cannot be measured, it is common practice to instead calculate the change in enthalpy (see Eq. 6). In accordance with Hess' Law, the change in enthalpy in chemical reaction is independent of the pathway taken, making it a state variable and negating the need for further analysis.

$$= \ + \ + + \tag{6}$$

Two assumptions are made regarding the system:

1. Pressure is constant (dp = 0)
2. Work done by the system comes in the form of pressure-volume work (W = -pV)

With these two assumptions, Eq. 6 is then simplified further (see Eq. 7), making the change in enthalpy within the system of combusting propellants equal to its change in total heat content.

$$= \ -++= \tag{7}$$

To calculate this change in heat content, various properties of the propellants must be observed: the heat of formation, heat of vaporization, and heat of reaction. The propellants are injected at a certain mass flow rate and mixture ratio, equating a certain number of moles for each the fuel and oxidizer to one unit mass of flow rate. Each mole of liquid propellant contains a certain amount of enthalpy needed to create the compound at a standard reference pressure and temperature, typically 1 atmosphere and 298.15 K, respectively. This amount of enthalpy, also known as heat of formation, is only given in a gaseous state, and because both the fuel and oxidizer are cryogenically stored in a liquid state, it is necessary to account for this phase change.

43

Therefore, the heat of formation of each liquid propellant component is coupled with its heat of vaporization.

The combustion process is an exothermic process, in that it releases heat, so high temperatures are created within the combustion chamber. Similar to the combustion process itself, these high temperatures produced by combustion further cause dissociation between the atoms of the various compounds of the combustion products. However, since mass is always conserved, the number elements constituting both the products and reactants (carbon, hydrogen, and oxygen) will remain constant.

Each compound, or species, within the combustion products has its own molar fraction, and therefore, its own amount of heat. The difference in total heat of formation between the products and the reactants is known as the heat of reaction. If it assumed that all the heat released from combustion is used to heat the combustion gases, the total change in enthalpy from each species in the combustion gases and from the reference temperature to the combustion temperature is equal to this total heat content.

Therefore, while we can reference the values for combustion temperature, average molar mass, and specific heat ratio from RPA, we may also calculate these values manually in order to provide a check. To do this, we observe the second law of thermodynamics, which states that the entropy, or the number of arrangement orientations of an isolated system, will increase until it reaches thermal equilibrium. Similarly, this also means that the Gibbs free energy, or the amount of energy available for conversion into mechanical work, will decrease until it reaches thermal equilibrium (see Eq. 8).

$$= +-$$

(8)

44

It is important to note that the assumption of constant pressure and temperature still hold throughout this equation. The goal of this process is to find the point at which this change in in Gibbs free energy is equal to zero (see Eq. 9)

$$= ++ \sum \hat{} \quad = \sum \hat{} \quad = 0 \tag{9}$$

Where:

G = Gibbs free energy
μ_j = Chemical potential per mole of the species, j
n_j = Langrange multipliers for each element, i

This equation introduces a new variable for each species, chemical potential, or μ_j. Chemical potential is a form of potential energy that may be either released or absorbed during combustion of the reactants. It is equal to the rate of change of Gibbs free energy per change in molar concentration of the combustion gases, or the change in Gibbs free energy during the extent of the reaction (see Eq. 10-11 and Figure 15).

$$\underline{\qquad} = \sum \quad = 0 \tag{10}$$

$$\tag{11}$$

Where:

$\hat{}$ = Gibbs free energy of formation per mole of species, j

45
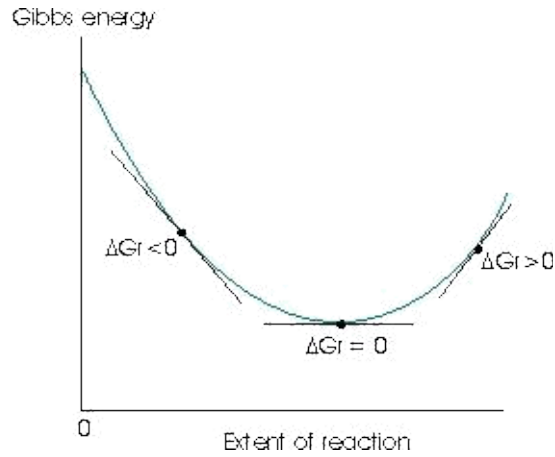
Figure 15: Graphic Illustration of Gibbs Free Energy throughout a Reaction

In order to solve this problem, a constraint must be introduced to the system. This constraint is in the form of the conservation of mass. From this constraint, the equation can then be modeled with a Lagrange multiplier (see Eq. 12).

$$(, \quad) = \Sigma^\wedge - \Sigma \qquad (\quad - \quad) = 0 \tag{12}$$

Where:

λ_i = Langrange multipliers for each element, i
a_{ij} = Stoichiometric coefficient for number of the atoms of element, i, per mole of the species, j
b_i = Assigned total mass of atoms of element, i
* = Atomic mass of element, i

Code was written in Matlab in order to iteratively calculate the proper combustion temperature and molar concentration of each species of the combustion gases (see Appendix E). The results and corresponding comparisons to the data extracted from RPA are in Tables 12a, 12b, and 12c.

Table 12a: Combustion Reactants vs Combustion Products

Combustion Reactants		Combustion Products		
Compound	Moles (Calc'd)	Compound	Moles (Calc'd)	Moles (RPA)
CH4	51.1937	H_2O	72.9364	72.8127
O2	71.2047	CO	37.5964	37.9751
		H_2	25.9545	25.8752
		CO_2	13.2910	13.2354
		OH	4.1608	4.2084
		H	3.2908	3.2658
		O_2	0.3675	0.3162
		O	0.3012	0.2902
		HCO	0.0529	0.0031
		HO_2	0.0096	0.0024
		COOH	0.0084	0.0016
		H_2O_2	0.0064	0.0008
		HCOOH	0.0001	0.0005
		HCHO	0.0002	0.0002
		Total	157.9762	157.9875

Table 12b: Elemental Mass Check between Reactants and Products

Element	Reactant Elements	Product Elements	Error
C	51.1937	50.8961	0.581%
H	204.7748	205.3177	0.264%
O	142.4093	142.4139	0.003%

Table 12c: Thermodynamic Properties

Property	Calculated	RPA	Error
T_c	3,383.6 K	3,367.1 K	0.488%
$\dot{m}$	19.61 g/mol	19.62 g/mol	0.081%
γ	1.21	1.17	3.248%

5.1.2 *Downstream Analysis*

After data extraction and back calculations were complete, the analysis continued. Throat and exit conditions were calculated under the assumption of isentropic flow (see Eq. 13 – 18).

$$\tag{13}$$

$$\tag{14}$$

$$\tag{15}$$

*As previously mentioned, the fluid will reach Mach 1 at the nozzle throat, so it does not need to be calculated

$$\tag{16}$$

$$\tag{17}$$

$$\tag{18}$$

5.2 Component Design

5.2.1 *Combustion Chamber*

The first piece of the engine we chose to design was the nozzle throat, as the design for both the combustion and thrust chambers rely on this value. However, the first step in this process involves the introduction of an extremely useful parameter, known as the "characteristic length", or L*. This parameter is not calculated, but rather chosen based off of the design of previous engines using similar propellants (see Table 12).

48

Propellant Combination	Combustion Chamber Characteristic Length (L*), in.
Chlorine trifluoride/hydrazine-base fuel	20-35
Liquid fluorine/hydrazine	24-28
Liquid flourine/liquid hydrogen (GH_2 injection)	22-26
Liquid fluorine/liquid hydrogen (LH_2 injection)	25-30
Hydrogen peroxide/RP-1 (including catalyst bed)	60-70
Nitric acid/hydrazine-base fuel	30-35
Nitrogen tetroxide/hydrazine-base fuel	30-35
Liquid oxygen/ammonia	30-40
Liquid oxygen/liquid hydrogen (GH_2 injection)	22-28
Liquid oxygen/liquid hydrogen (LH_2 injection)	30-40
Liquid oxygen/RP-1	40-50

Table 12: Combustion Chamber Characteristic Length

Since the LO_2/LCH_4 propellant has largely gone unused until recently, it obviously does not have an experimentally evaluated characteristic chamber length. For these purposes, it was necessary to make an educated estimate as to what value we should use. Looking at the trend of characteristic lengths for the different fuels, along with their corresponding energy densities, one can deduce that a higher energy density generally requires a lower characteristic length. We therefore chose a value of 90 cm (35.4 in) for our propellants.

Since the pressure and temperature of the fluid at different points along the nozzle are dictated by the isentropic flow process, along with the fact that the mass flow rate has been chosen as an input, the throat area is then calculated (see Eq. 19).

$$\tag{19}$$

This value subsequently yields the throat diameter, as well as the overall chamber volume (see Eq. 20).

$$* = \underline{\quad\quad}$$

After calculating the throat area and diameter, we could then proceed with the sizing of the combustion chamber. Two important design parameters are the chamber length and the contraction ratio, which is the ratio of chamber area to the nozzle throat area (see Figure 16).
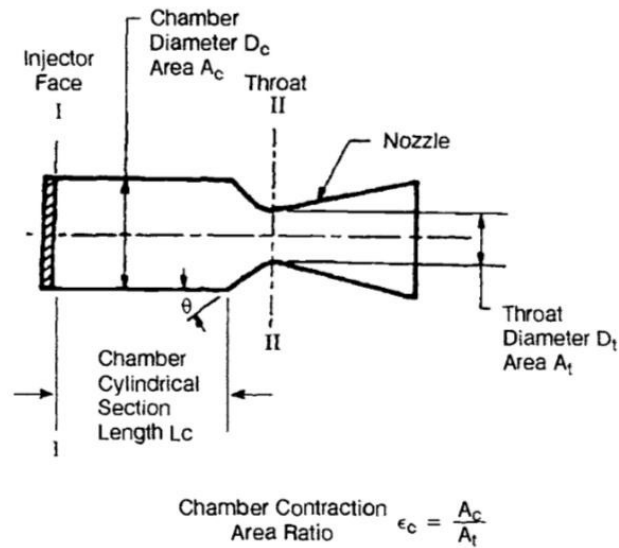
Figure 16: Cylindrical Combustion Chamber Elements

Data plots from previous engines were used to calculate both of these values (see Figures 17 and 18). Similar to the calculation of the preliminary outputs (optimum O:F ratio, chamber temperature, molar mass, and specific heat ratio), it was important to extract the data from these plots and formulate algorithms in order to adjust the design values instantaneously.
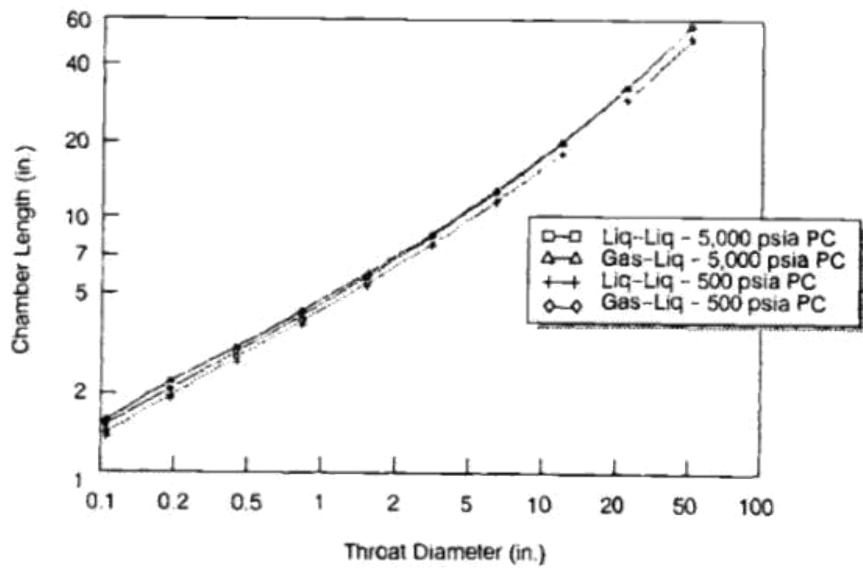
Figure 17: Chamber Length vs. Throat diameter relationships
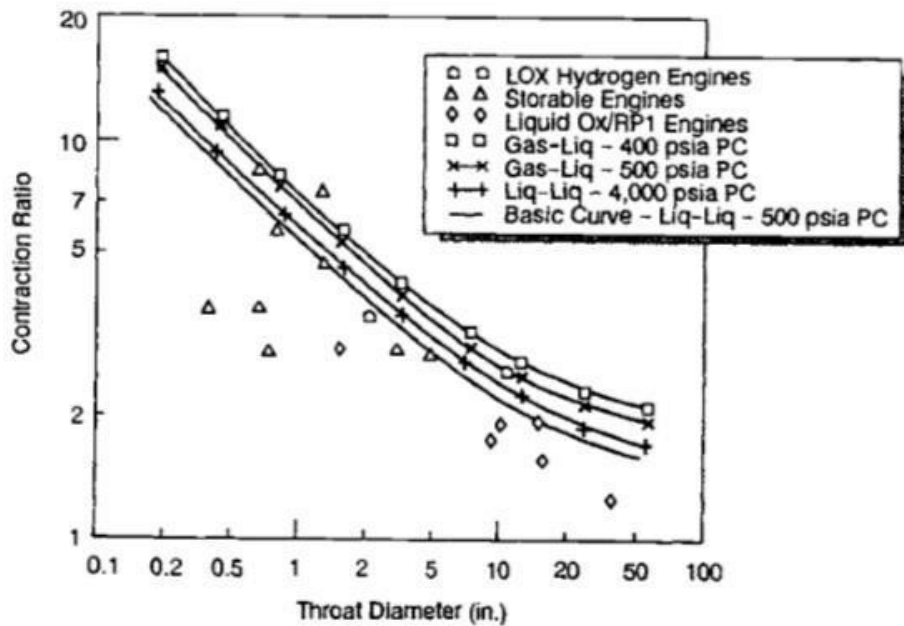
Figure 18: Contraction Ratio vs. Throat Diameter Relationships

Among the most important parameters for determining the chamber length is the condition of the propellants. The chamber must have sufficient length to achieve the proper the vaporization and reaction of the propellants, as well as maintain its characteristics as a pressure vessel.

51

Additionally, a smaller diameter increases the likelihood of combustion stability, while a longer length will aid in providing an adequate amount of turbulence for mixing and reaction. A piece of this design includes the contraction angle, or β, which plays a role in determining the exact length of the chamber (see Eq. 21).

$$L_c = \frac{V_c - \frac{\pi}{3}\left(R_c^3 - R_t^3 + \frac{24}{\tan\beta}\right)}{\pi R_c^2 \tan\beta} \tag{21}$$

Once the proper contraction angle has been determined, the total surface area of the combustion chamber can also be computed (see Eq. 22).

$$A = 2\pi R_c \sqrt{L_c + \csc(\beta -)} \tag{22}$$

5.2.2 Nozzle

As previously mentioned, the propellants combust and the gas heats up to an optimum temperature (and therefore an optimum pressure) before travelling through the convergent section of the combustion chamber where it is accelerated to a sonic velocity. At this point, it has reached the minimum cross-sectional area, called the throat, which can also be classified as the entrance of the nozzle section of the engine. From this point forward, the fluid then expands and loses heat, further turning its thermal energy into kinetic energy. An optimum expansion ratio will ensure that the gases are expanded to a point where their inherent pressure matches that of the ambient atmosphere.

Knowing the expansion ratio, throat radius, and exit radius, we can also calculate the length of the nozzle for a conical geometry (see Eq. 23 and Figure 19)

$$= \frac{(\sqrt{\quad} - 1) + 0.382\ (\sec\ - 1)}{\tan} \qquad (23)$$
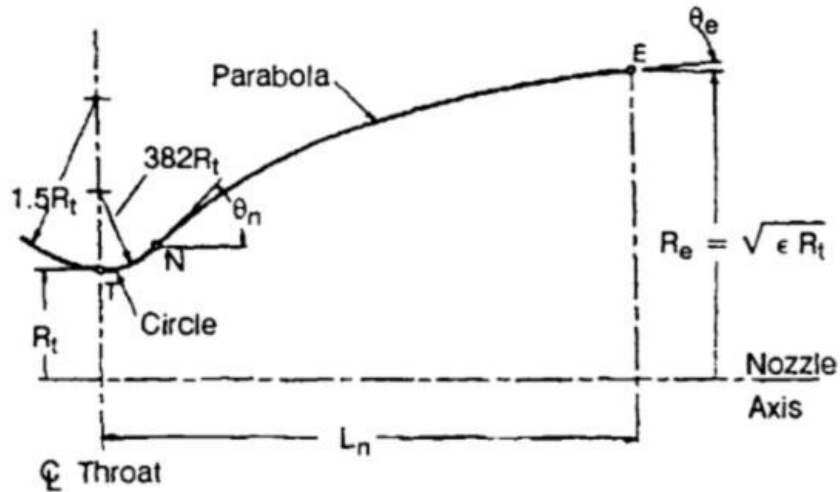
Figure 19: Parabolic Geometry of a bell nozzle

The design of the parabolic contour of the thrust chamber is somewhat complicated. First, an incoming circular arc from the convergent portion of the combustion chamber reaches the throat at a point where it is precisely tangent to the direction of the flow. This first circular arc is defined as having a radius of 1.5 . Next, a smaller circular arc continues from this same point, defined as having a radius of 0.382 . This arc continues until a certain point, designated "N", where the parabolic curve takes over and continues until a point at the exit of the nozzle, designated "E". Using a coordinate system based on the centerlines of the throat and thrust chamber, this point is calculated using the initial and exit angles of the parabolic arc, designated θ_n and θ_e, respectively. These angles are found as a function of the expansion ratio and fractional length (see Figure 20).
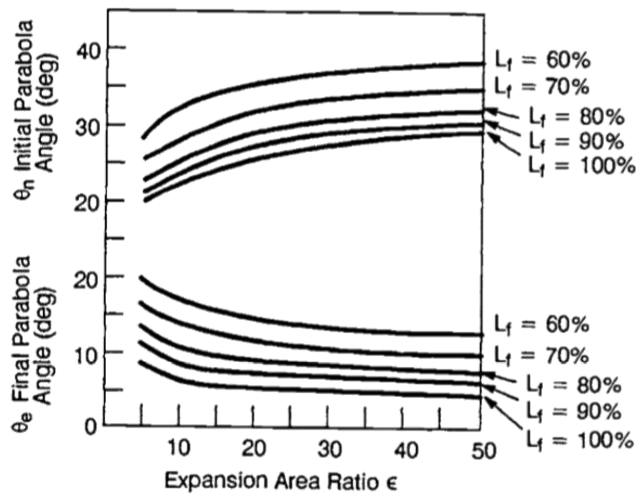
Figure 20: Initial and Exit Angles of a nozzle parabola

Once these angles are found, the x- and y-coordinates for points "N" and "E" can be calculated using Eq. 24-27.

$$= 0.382 \ \sin \tag{24}$$

$$= + 0.382 \ (1 - \cos \ ) \tag{25}$$

$$= \tag{26}$$

$$= \tag{27}$$

The final piece of the contour design is calculating the parabolic curve that constitutes the bulk of the chamber nozzle, which can be calculated using Eq. 28-30. It is important to note that this equation begins with the y-axis oriented a distance N_x from the centerline of the throat.

$$= + \tag{28}$$

$$-(\quad , \quad -^2 \quad) \tag{29}$$

$$= -(^2) \tag{30}$$

54

Calculated chamber and nozzle components, along with their corresponding comparisons to the data extracted from RPA, are listed Table 13. Given the nature of the calculations, discrepancy between our values and the values extracted from RPA was far more prevalent than previous analysis. However, error remained under 10%.

Table 13: Calculated Geometric Engine Data vs RPA Data

Component	Calculated		RPA	Error
	Metric	**English**		
V_c	796,450.99 mm^3	44.18 in^3	721,111.16 mm^3	9.459%
D_c	72.96 mm	2.88 in	73.18 mm	0.294%
L_c	177.19 mm	7.48 in	189.91 mm	6.699%
P_t	4.0357 MPa	585 psi	4.0789 MPa	1.059%
T_t	3,063.25 K	6,089.10 ^{o}R	3,153.41 K	2.859%
A_t	801.235 mm^2	1.247 in^2	796.451 mm^2	0.597%
M_e	3.227	3.227	3.175	1.587%
V_e	2,941.996 m/s	9,652.218 ft/s	3,008.776 m/s	2.220%
P_e	0.1013 MPa	14.696 psi	0.1013 MPa	0.025%
T_e	1,621.54 K	2,918.78 ^{o}R	1,791.22 K	9.473%
A_e	7,152.978 mm^2	11.087 in^2	7,392.859 mm^2	3.245%
ε	8.927	8.927	9.227	3.245%
L_n	95.57 mm	3.76 in	104.71 mm	8.732%
θ_n	20.25^o	20.25^o	20.46 ^{o}	1.016%
θ_e	14.73^o	14.73^o	14.72 ^{o}	0.096%

After calculating all chamber and nozzle components, the design of the combustion chamber and nozzle components can be seen in Figure 21. For previously mentioned structural and financial purposes, the combustion chamber was "blown out" from a cylindrical shape to a near-spherical shape, while maintaining the same volume stay time to ensure proper and efficient combustion of the propellants.

Dc = 4.26 in   De = 1.25 in   De = 3.81 in

Lc = 4.70 in   Ln = 4.12 in
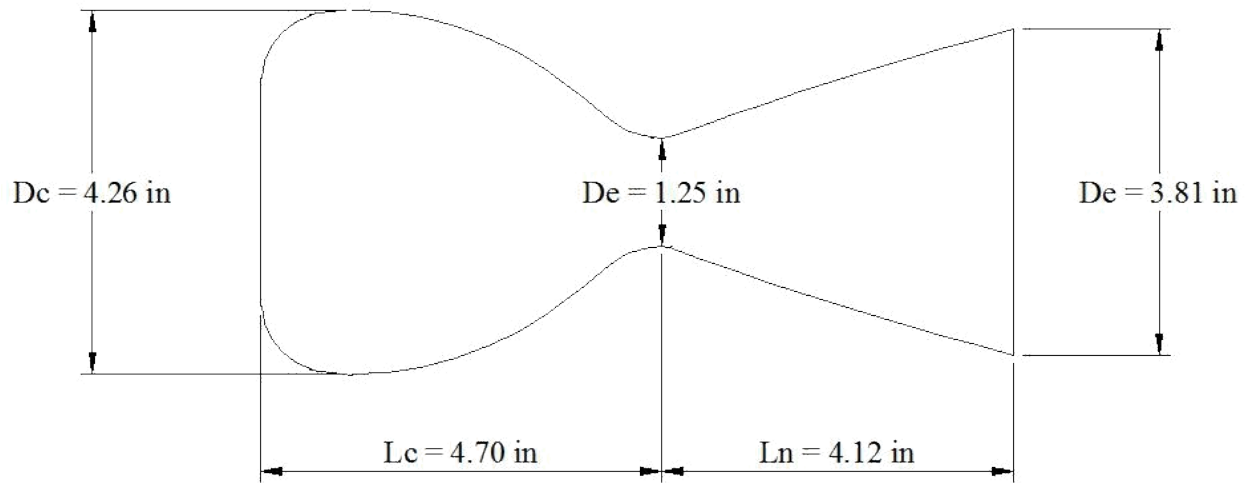
Figure 21: Combustion Chamber and Nozzle Design

5.2.3 Cooling System

Due to the extremely high temperatures in the combustion chamber and thrust chambers, it is imperative that both be cooled in order to prevent material failure. Initially, we calculated the convection and radiation heat transfer in order to determine the amount of heat it is required to dissipate through means of cooling. Once the total temperatures were calculated, the goal was to dissipate the maximum amount of heat using pure regenerative cooling. Because there was an excess of heat to dissipate surrounding the combustion chamber, the remaining heat was distributed through film cooling along the chamber walls. However, a minimal amount of film cooling is desired in order to avoid substantial losses in performance from burning propellant purely for cooling reasons and adding weight to the overall system.

5.2.3.1 Cooling-Convective Gas Side Heat Transfer

Heat transfer analysis of the chamber and nozzle can be performed using the Bartz method (see Eq. 31-39).

$$= \frac{4}{9 - 5} \tag{31}$$

The Prandtl number is a dimensionless number that is used to define the momentum over the thermal diffusivity, which, bases on the specific heat ratio of the fluid, illustrates its heat capacity.

$$\frac{1 + \frac{1}{3}(\frac{-1}{2})2}{2} \tag{32}$$

The adiabatic wall temperature of the combustion gases is a function of Prandlt number, gamma, and the Mach number at a given location long the length of the combustion chamber.

$$= [2 \frac{1}{(1 +} \frac{-1}{2}^{1 -0.68})+2] \frac{-1}{(1 +}^{-0.12} 2] \tag{33}$$

The sigma value is a correction factor developed through experience with turbulent boundary layers, which eventually develops the hot gas-side head transfer coefficient shown in Eq. 36.

$$= \frac{}{(-1)} \tag{34}$$

$$= 46.6 \; 10^{-6} \; 0.5 \; 0.6 \tag{35}$$

$$h = \frac{0.026}{0.2 \; 0.6}^{0.2} \; \frac{}{}^{0.8} \frac{0.1}{} \; \frac{0.9}{} \tag{36}$$

Once the hot gas side heat transfer coefficient is calculated, we could then determine what the required convective heat flux needed to be in order to ensure that the temperature would under that of the thermal expansion rate for Cobalt Chromium.

$$= h \left(\quad - \quad \right) \tag{37}$$

5.2.3.2 Radiation Gas Side Heat Transfer

$$= \frac{}{[1 - (1 -)(1 -)]} \tag{38}$$

$$\left(\quad - \quad ^4 \right) \tag{39}$$

Once the convection and radiation heat flux are calculated you simply add the two together in order to achieve a total heat flux along the location of the combustion chamber. The numbers acquired from the equations above are shown in Appendix C and D. The nozzle throat and contraction section temperatures are listed in Table 14.

5.2.3.3 Applied Heating Outputs

Table 14: Applied Heating at Chamber Inlet and Throat

Results of Thermal Analysis								
Location	**Radius**	**Conv. heat coefficient**	**Conv. Heat flux**	**Rad. Heat flux**	**Total heat flux**	$\mathbf{T_{wg}}$	$\mathbf{T_{wi}}$	$\mathbf{T_{wc}}$
in	in	$Btu/(in^2\text{-s-R})$	$Btu/(in^2\text{-s})$	$Btu/(in^2\text{-s})$	$Btu/(in^2\text{-s})$	$_\circ R$	$_\circ R$	$_\circ R$
3.532	1.208	0.0023	1.7392	0.2559	1.995	5296	5296	5163.02
6.291	1.211	0.0019	1.5331	-0.0263	1.5068	4907.66	4907.66	4813.19
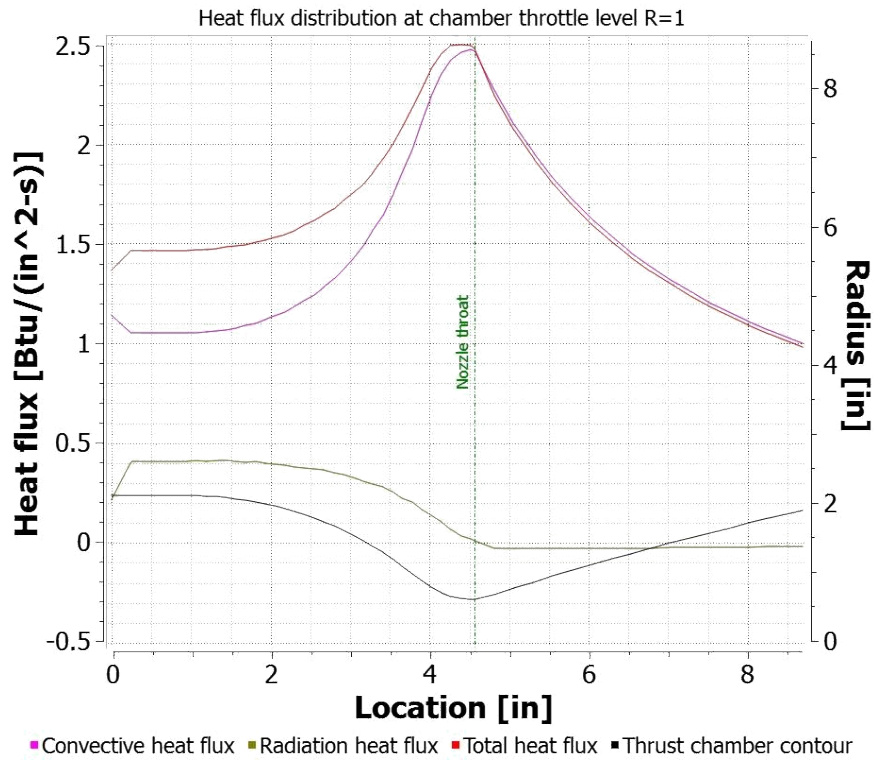
Figure 22: Applied Heat Flux along the Chamber Wall
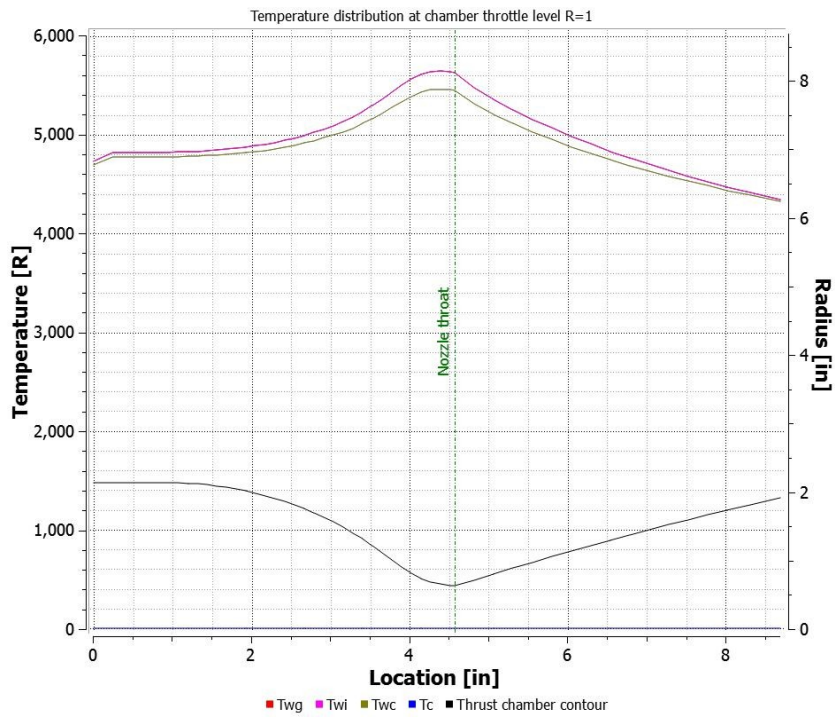
Figure 23: Applied Temperature Distribution along the Chamber Wall

59

Figure 22 and 23 above show the convective heat flux, radiation heat flux, total heat flux, gas side temperature, and wall side temperature of the combustion chamber and nozzle at the current configuration. It is important to note the 2-Dimensional contour of the engine is shown at the bottom of the graph which gives a clear visualization of what the heat is doing at each location of the engine. Temperature and heat flux stay relatively constant in the combustion chamber while they both rise during contraction, although once sonic flow is reached at the throat they both dive exponentially. It is important to notice that the majority of the heat flux comes from convection not radiation which was initially more intuitive. Also radiation only exits in the combustion chamber and is neutralized upon entry of the nozzle divergent section.

The following graph was then created in order to show an up close depiction of the temperature characteristics throughout the nozzle section of the rocket engine.
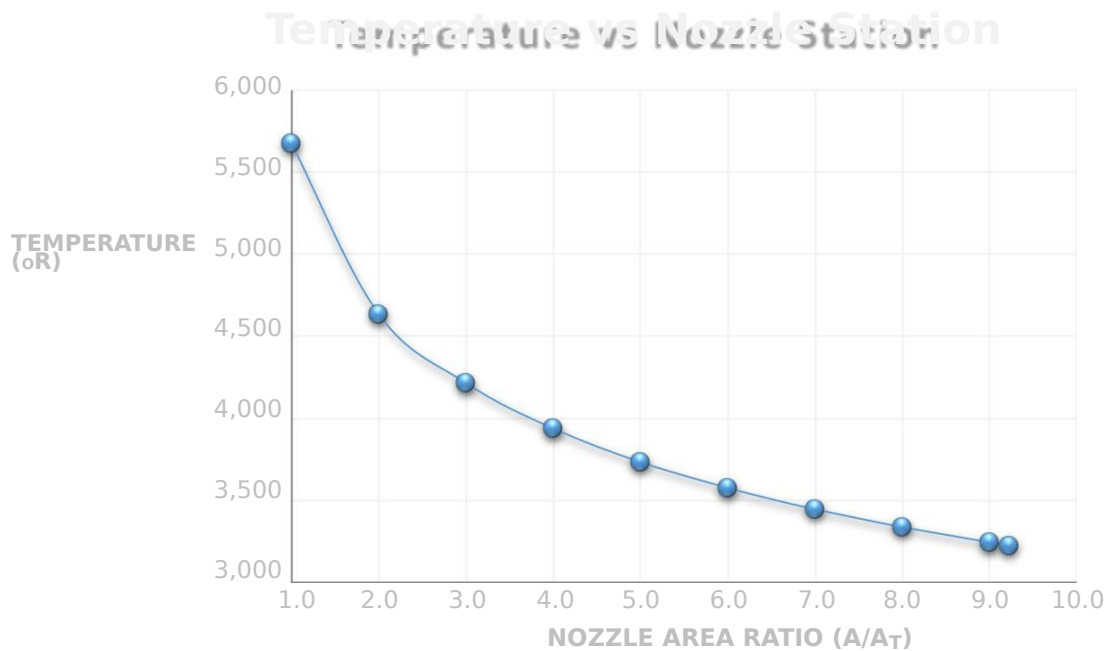
Figure 24: Temperature Variation in Nozzle

Table 15: Thermal Properties of Cobalt Chromium

Property	Min Temp (°F)	Max Temp (°F)	Value
Coefficient of Thermal Expansion	36	900	7.6 x 10-6 in/in °F
	900	1800	8.4 x 10-6 in/in °F
Thermal Conductivity		36	90 Btu/(h-ft^2-°F/in)
		540	125 Btu/(h-ft^2-°F/in)
		900	153 Btu/(h-ft^2-°F/in)
		1800	229 Btu/(h-ft^2-°F/in)
Maximum Operating Temperature			2100 °F
Melting Range			2460 - 2600 °F

5.2.3.4 Regenerative Cooling

From the heat transfer characteristics calculated above it is apparent that more cooling is required through means of regenerative cooling. The system slices the combustion chamber and nozzle into sections in order to determine the required heat flux to dissipate throughout the rocket engine. The following method is shown from Eq. 40 – 44.
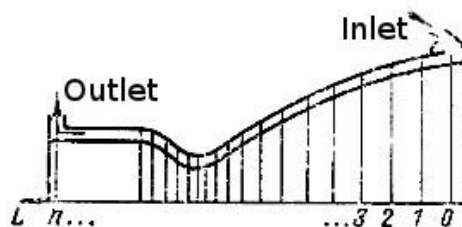
Figure 25: Cooling Flow around the Chamber and Nozzle

$$= 2 \quad (\qquad \underline{\qquad} \quad)$$
$$h = $$
$$= 0.0185 \quad {}^{0.8} \qquad \qquad {}^{0.4} \, (\qquad)$$

(40)

(41)

(42)

Once the change in temperature at each section is calculated the next step is to create coolant passages along the chamber walls that can be analyzed and treated as hydraulic conduits. Finally once the passage diameter is finalized, the pressure drop along the coolant fluid flow can be calculated in order to determine a new tank pressure. The desired coolant passages will be circular for the least amount of pressure drop, therefore the ε_f factor shown in Equation 43 will equal zero.

$$= (0.0032 + \quad \underline{\quad 0.221 \quad})$$
$$_{0.237}$$

(43)

$$\Delta = \frac{\frac{1}{\quad} \quad \frac{2}{\quad}}{2}$$

(44)

The Regenerative cooling design will be most critical where the initial pressure chamber pressure has an increasing slope induced by the nozzle. The design starts at the nozzle exit with 100 tubes at a diameter of 3 mm. Once the Fuel runs axially up the chamber to the location of 6.229 in, the Fuel converges into 50 tubes at a diameter of 3.25 mm in order to drop the pressure, increase the velocity, and increase the heat transfer to the coolant fluid. Once the end of the critical contraction point of the nozzle is reached it is then diverged once more into 100 coolant tubes in order to regain some of the lost pressure before being injecting into the fuel manifold of the injector plate.

5.2.3.5 Film Cooling

The following equations are used in order to calculate the film temperature along the chamber walls in the direction of thrust as a function of mass flow rate as it enters the combustion chamber. Notice that mass flow rate is provided as a function of the propellant vaporization characteristics meaning that the mass flow rate will decrease as more propellant is vaporized and turned to gas from the hot combustion gases. The film coolant goes through three distinct phases that have different thermal properties being heating, vaporization, and mixing.

$$\underline{\qquad} = \frac{2}{} \tag{45}$$

$$\underline{\quad} \quad \frac{2}{} \tag{46}$$

After film and regenerative cooling was applied, the heating new distributions could be seen in

Figures 29 and 30. Ideally, the cooling design would want to dissipate as much heat through the

fuel so that you do not lose any efficiency in the combustion process through film cooling. A

design of 30% Fuel Film Cooling (FFC) was selected due to constraints of the 3D printer. The

DMLS Printer (EOS 270) has an internal diameter limit of .030in, which forced the use of a

minimum of 30% FFC to meet the internal diameter.
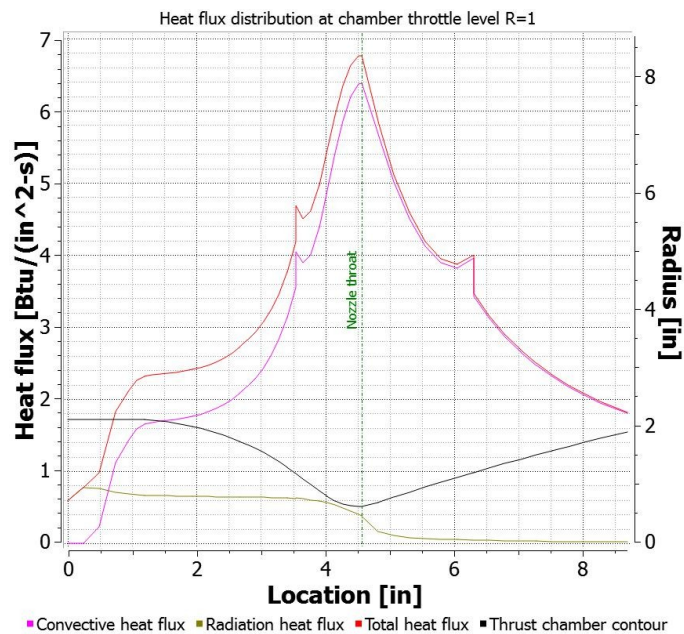
Figure 26: Heat Flux along the Chamber Wall with Film Cooling Design

Figures 26 and 27 show the new heat transfer distribution along the chamber walls once

the final regenerative and film cooling designs were applied. It is important to note the new

maximum temperature, which has decreased from 5500 °R to 1488 °R, well below the final

thermal expansion rate of Cobalt Chromium as defined by GPI. The blue line in Figure 29 shows

the fuel coolant temperature increasing from right to left as it travels in the retrograde of the hot

gases exiting the nozzle. Lastly, the spike in heat flux in the center of the graph shows where the

coolant flow transitions from 100 tubes to 50 tubes then back to 100 tubes before entering the

fuel manifold in the injector.
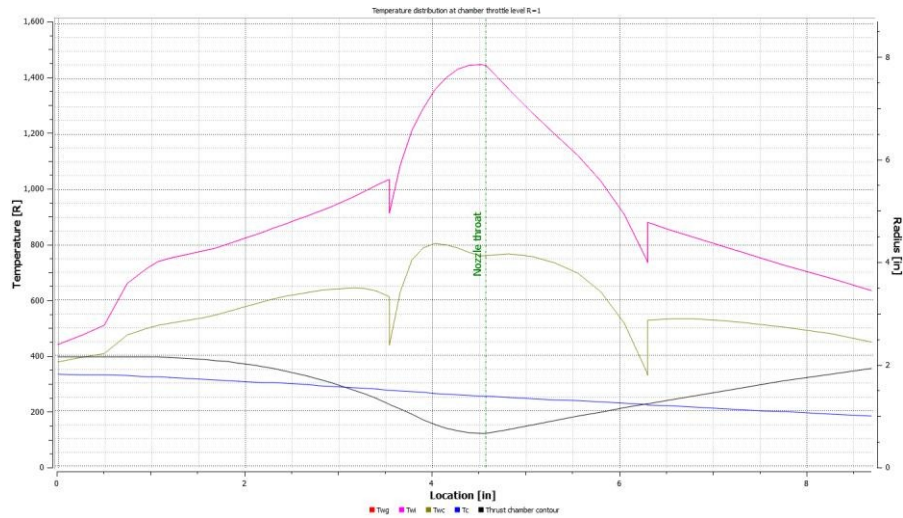
Figure 27: Temperature Distribution along the Chamber Wall with Film Cooling Design

5.2.4 Injector

For orifice elements, the injection area and orifice size can be calculated using Equations 47 and

48.

$$= \frac{\dot{w}}{\sqrt{\Delta}}$$

$$= \left(\frac{3.627}{\Delta \cdot 2}\right) \frac{2.238}{2}^{0.25}$$

Where:
$\dot{w}$ = Weight flow of propellant component
K = Head loss coefficient
N = Number of orifices
ρ = Density of propellant component
Δp = Pressure drop across injector plate (typically 20%)

(47)

(48)

65

Given the dimensions of the combustion chamber, the diameter of the entire injector plate was required to be under 4.2 inches in diameter. It was also important for the length of the injection channels connecting the manifolds to the at least 4 times the diameter of their corresponding orifice in order to maintain laminar flow and prevent any reverse flow. Using a similar principle, the areas for each the oxidizer and fuel injection manifolds were calculated at 4 times the total orifice area that they feed. Given the nature of impinging triplets, it was desirable to design the impinging distance from the face of the injector plate to be about one half of one inch. It was also desirable to design the impinging angles between the oxidizer and fuel to be between 25 and 45 degrees to ensure proper mixing while maintaining axial flow. Due to the high constraint for space and requirement for laminar flow within the channels, the impinging distance was designed at 0.4544 inches, while the impinging angles were designed at 27 degrees on each side of the center CH_4 orifice. Finally, it was also necessarily to design all orifices to be above the minimum tolerance for the 3D printer, which is set at 0.02 in.

The outer film coolant ring feeds 30% of the mass flow of the fuel, while the remaining 70% is divided among individual manifolds feeding their own single orifices. Oxidizer mass flow rate is divided evenly between the inner and middle rings (see Figure 28).

Figures for the injector plate are as follows:

Table 16: Injector Plate Geometric Figures

Ring	Propellant Component	Total Orifices	Total Orifice Area (in^2)	Orifice Area (in^2)	Orifice Diameter (in)	Manifold Area (in^2)	Manifold Diameter (in)
Inner	Oxidizer	8	0.0605	0.0038	0.0694	0.1210	0.3926
2	Fuel	8	0.0251	0.0031	0.0632	0.0126	0.1265
3	Oxidizer	8	0.0605	0.0038	0.0694	0.1210	0.3926
Outer	Fuel	14	0.0108	0.0008	0.0313	0.0431	0.2342
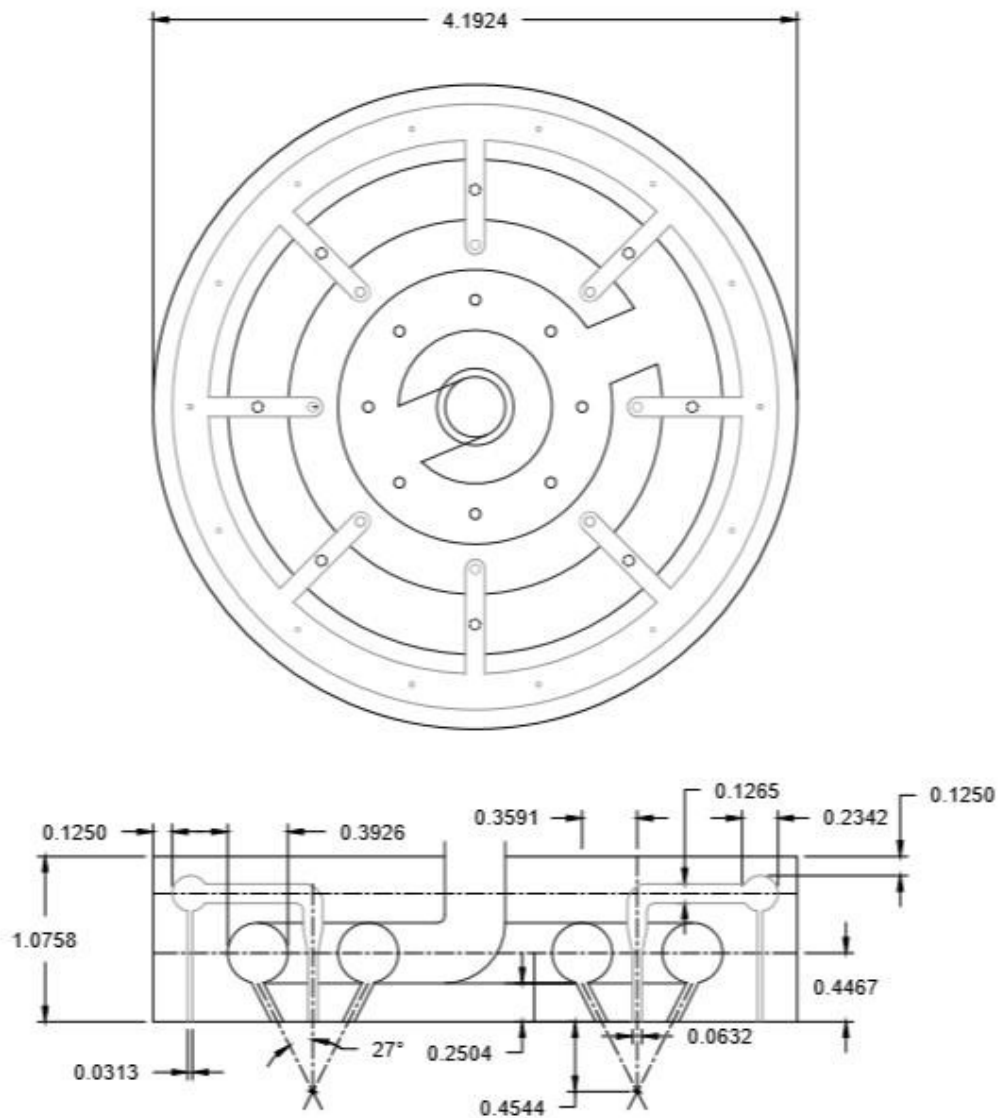
Figure 28: Injector Orifice Design (all dimensions in inches)

Figure 29: SDSU Rocket Club Injector Device

A simple and cheap design for the ignition device is to utilize a small solid rocket motor with small holes so that it will ignite radially within the chamber. This apparatus will attach to a stand inserting it directly into the combustion and thrust chambers. Once combustion occurs, the exhaust gases from the engine will push the igniter apparatus away from the test stand. This design allows for the combustion chamber, nozzle, and injector device system to be combined into one component for ease of manufacturing while utilizing DMLS manufacturing processes. The image shown in Figure 29 is a simple solution to ignite the propellants in order to validate our designs, having been previously used by SDSU. It should be noted here that this solution is not feasible for Mars descent or ascent application, so a more complex igniter can be designed at a later time in order to make this engine feasible for flight.

5.2.6 Propellant Feed System

The propulsion system will be pressure-fed using helium as the gas that will directly pressurize the propellant tanks. The amount of pressurant required has been calculated based on tank pressure, propellant volume, pressurant temperature, and compressibility of the pressurant (see Eq. 49).

$$= \quad \frac{}{} \tag{49}$$

Where:

W_g = Required weight of the pressurant gas
P_t = Tank pressure
V_t = Tank volume
Z = Compressibility factor of the pressurant gas (used as 0.95 for gaseous helium)
R_g = Specific gas constant of the pressurant gas
T_g = Storage temperature of the pressurant gas

The tank volume required for the pressurant gas could then be calculated using the simple relationship in Eq. 50.

$$= \quad \frac{}{} = \frac{}{} \tag{50}$$

With a pressurant gas tank pressure of 3,500 psi and stored at a room temperature of 298.15 K, these equations yield a minimum weight requirement of 1.22 lb and total volume of 838.70 in^3. Even when considering margins of excess amounts of pressurant in case of testing issues, these values are very manageable given the cost and availability of helium.

5.3 Engine Parameters and Performance Figures

5.3.1 Inputs

$\underline{L}^{*} = 35.43$ in

$P_c = 1,040$ psi
$P_a = 14.7$ psi (SL)
$\dot{m} = 6.83$ lbm/s
$\epsilon_c = 5.21$
$\theta_c = 40°$
$L_f = 80\%$
$\alpha = 15°$

5.3.2 Performance Data

Table 17: Ideal Performance Data vs Estimated Delivered

	Thrust (lbf)	C (ft/s)	C* (ft/s)	C_f	Isp (s)
Ideal Performance	2,058.00	9,871.31	6,128.33	1.61	306.81
Estimated Delivered Performance	2,009.40	9,459.70	6,035.58	1.57	294.02

70
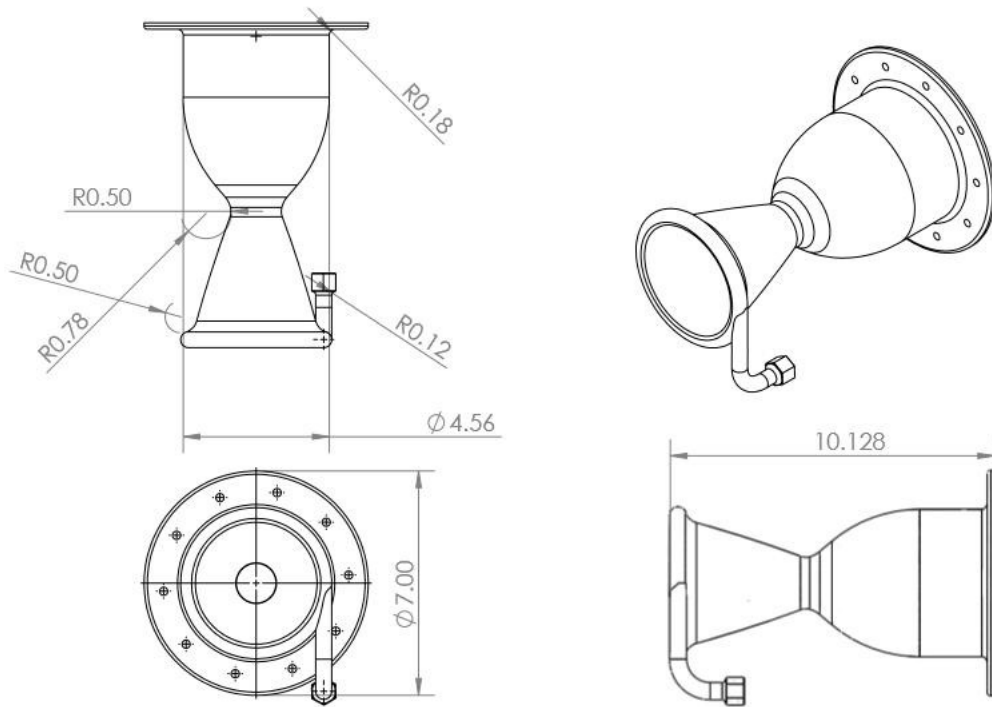
5.4 CAD Models

Figure 30a: 2D CAD Models of the Leon 1 Rocket Engine
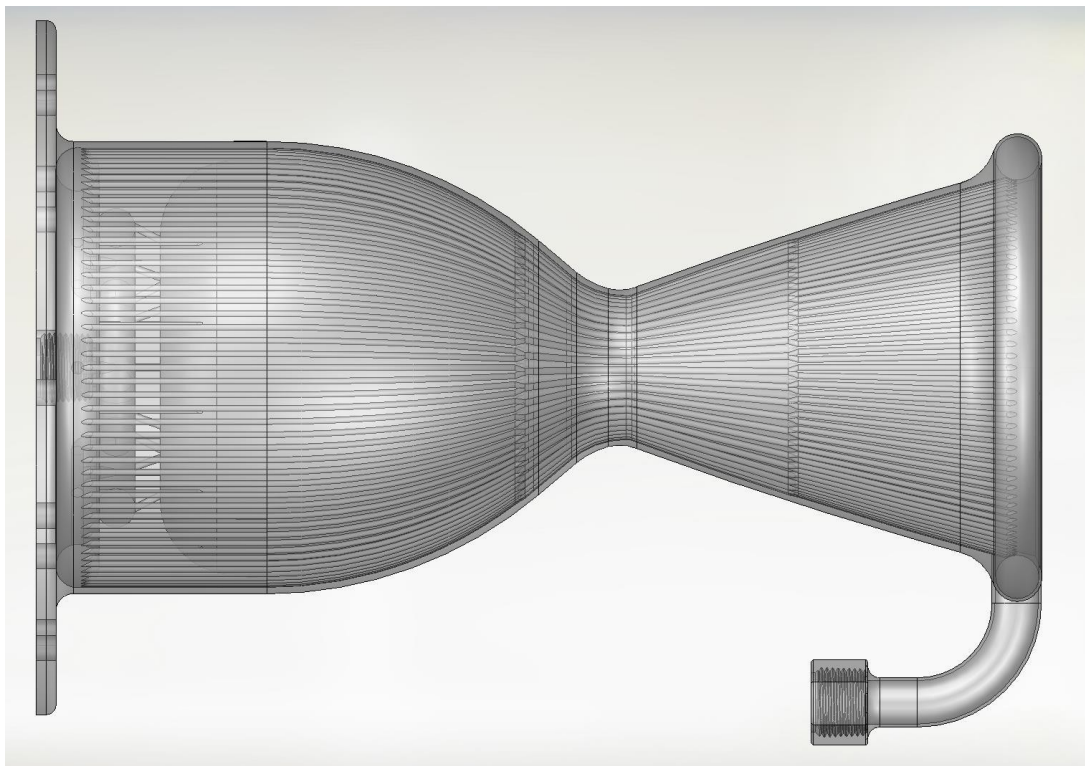
Figure 30b: 3D CAD Model of the Leon 1 Rocket Engine

Figure 30c: 3D CAD Model of the Leon 1 Rocket Engine

5.5 CFD Simulations

Computational Fluid Dynamics (CFD) simulations were performed using ESI. The simulations

were run as turbulent, using the Baldwin-Lomax model. All fluid properties, including molecular

mass, pressure, temperature, and ratio of specific heats, were input to match those of the combustion

gases calculated and checked earlier in the design process. The exit properties for pressure and

temperature were subsequently set to 1 standard atmosphere. The engine itself was

broken up in four sections: the combustion chamber, the nozzle, the axial exhaust, and the ambient atmosphere. Distribution of the grid points were oriented so that the walls of the engine could be closely monitored. Additionally, for the most accurate simulations possible, 500 grid points were used along each geometric line, creating a total number of 1,000,000 grid points within the entire mesh. The output data from the simulations validated the previous calculated performance values.
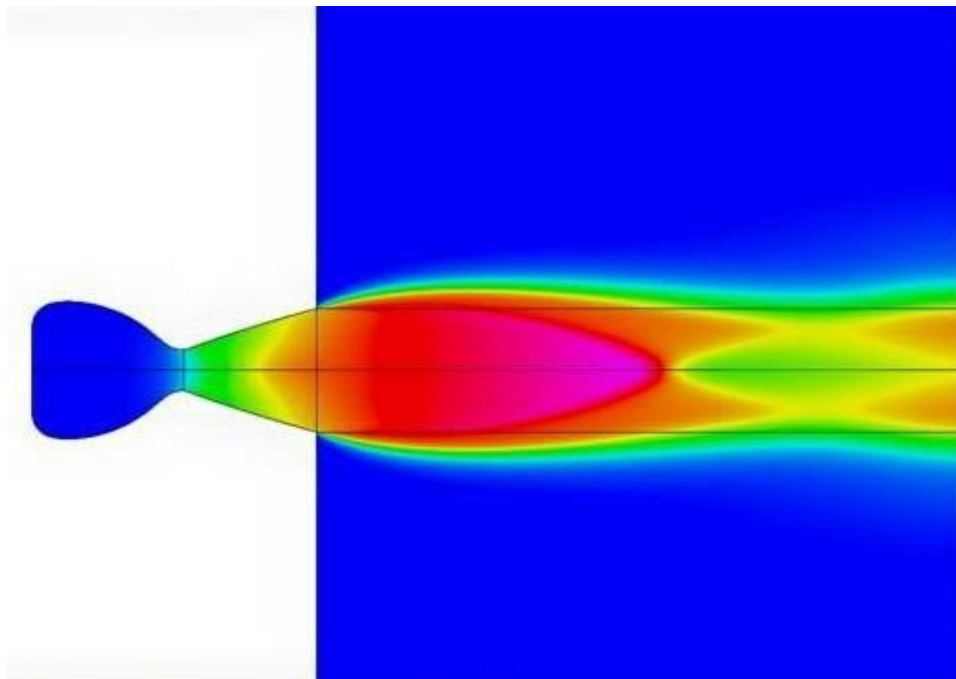
Figure 31: CFD Simulation Illustrating Mach Variation

CFD Outputs:

Exit Mach: 3.1
Exit Temperature: 1,800 K
Exit Pressure: 0.110 MPa

6.0 MANUFACTURING AND COST

Correspondence with GPI Prototype and Manufacturing yielded final quotes of $1,373.05 for the plastic version of the engine, which has been used to execute a hydraulic flow test, and $12,979.87 for the full Cobalt Chromium model, which will be used to execute the static test (see Figure 32). Fundraising has been a collaborative effort between crowdfunding through the website GoFundMe.com, which has raised over $2,500 alone, as well as Associated Students through SJSU, which has approved our team for the amount of money required to print the engineering plastic version for the hydro test.

GPI PROTOTYPE & MANUFACTURING SERVICES™

940 North Shore Drive • Lake Bluff, Illinois 60044
Phone: 847-615-8900 • sales@gpiprototype.com

Quotation

To: San Jose State University SEDS
1 Washington Sq
San Jose , CA 95192

Quotation No.:	64523 - REV4
Date:	4/7/2015
Inquiry Date:	3/6/2015
Terms: *(with approved credit)	Net 30*
Supplier Number:	
Ready to Ship:	TBD
F.O.B:	Our Dock

Quantity	Description	X	Y	Z	Material	Layer	Price
		Units		MM			
		*Does not indicate build orientation					
	L3_final_30percent_14_orifices_cut_1						
	L3_final_30percent_14_orifices_cut_2						
1	DMLM lot charge for qty one of each part listed above				MP1	40µm	$12,979.87
	Charge for welding						$50.00
	L3_final_30percent_14_orifices.						
1	SLA build charge for 1 of the above listed part in Accura ClearVue						$1,373.05
	Finish to be rapid clear (some build lines still visible)						
	SLA Lead Time: 7-10 Days						

Figure 32: Cobalt Chromium and Plastic Engine Manufacturing Quotes from GPI

7.0 HYDRO AND STATIC TESTING

Before the static test can be executed, it was important to test both the cooling and injection systems with a hydro flow test, using air-pressurized water as a replacement for the propellant components. This test ensured that all channels designed within the structure of the engine

allowed steady flow, while also ensuring that the engine was printed properly and thoroughly. A reusable test stand was constructed out of plywood, using an acrylonitrile butadiene styrene (ABS) water tank, brass pipe fittings, plastic nylon-reinforced tubing, and a single pressure regulator rated to 300 psi (see Figure 33a). During the test, red dye was used in order to allow for more accurate observations (see Figure 33b). Total cost of the stand was $320.

Figure 33a: SEDS SJSU Hydro Flow Test Stand
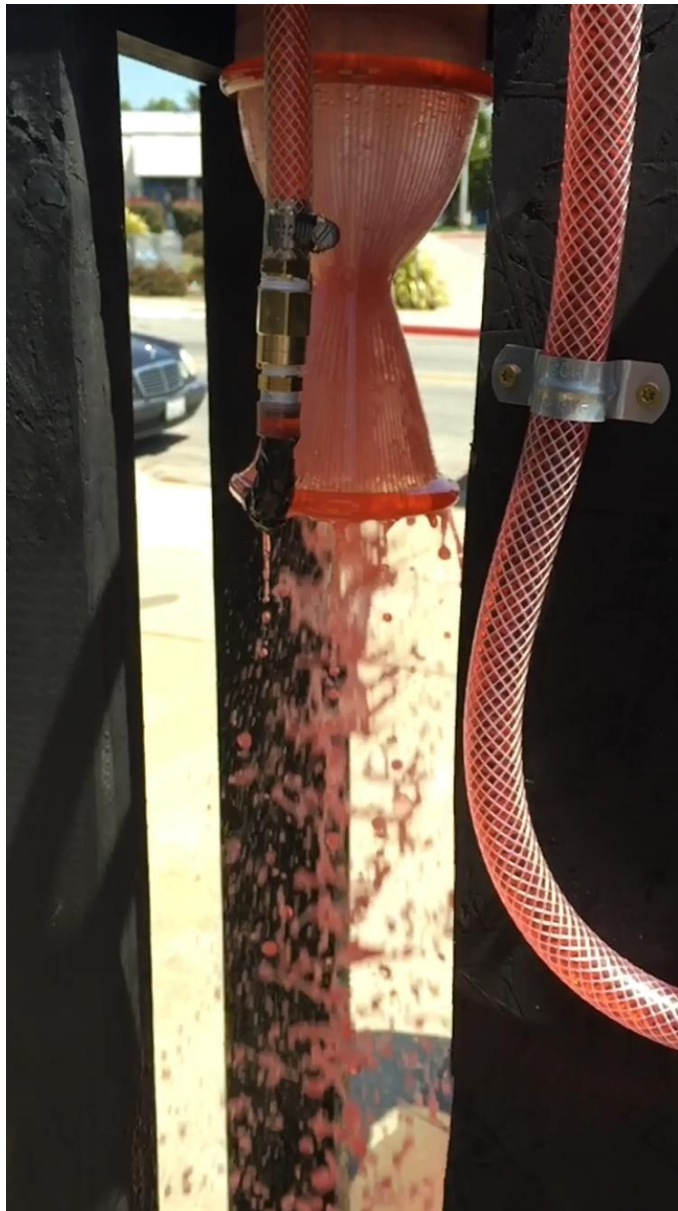
Figure 33b: SEDS SJSU Hydro Flow Test Stand

After the most updated iteration of the Leon 1 is delivered, we will perform an additional

hydro flow test. Assuming this test goes as planned, we will then look toward the static test of

the Cobalt Chromium version of the engine. However, this will require additional funding and/or

sponsorship. We have been in talks with GPI to sponsor the engine at about 90% of the cost,

coupled with the funds raised by SEDS SJSU to this point. As previously mentioned, we have also been in communication with SEDS at USCD in order to utilize the static test stand which they have built and previous used to test a rocket engine of similar scale. The basic test stand schematic can be seen in Figure 34.
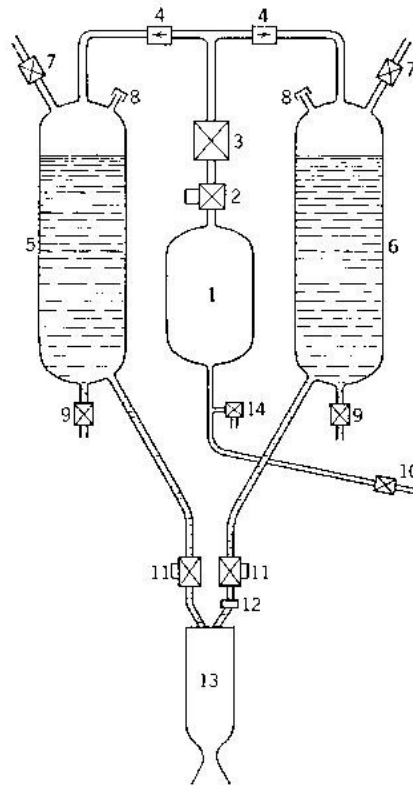
Figure 34: Schematic Diagram of a Gas Pressure Feed System

The basic static test stand consists of two propellant tanks, one for each liquid oxygen and liquid methane, as well as a tank for helium. Attached to the tanks are various propellant feed lines, pressure regulators, pressure gauges, relief valves, and feed valves. However, the tanks used by UCSD, along with their corresponding pressure regulators, have been found to be inadequate for our design, and therefore will need to be replaced and tested prior to the static fire. A budget for these items has been formulated and can be found in Table 18.

Table 18: Itemized Budget List for Static Test Stand Enhancements

Item	No of Items	Manufacturer	Min Pressure/Force (psi/lbf)		Min Temperature (K)	Cost per Item ($)
Metal Engine	1	GPI				$12,979.87
Weld	1	GPI				$50.00
Plastic Engine	1	GPI				$1,373.05
UCSD Test Stand Rental	1	UCSD				$500.00
Pneumatic Pressure Regulator	2	Aqua Environment	0-6000	psi		$593.00
Helium Supply Tank	1	Praxair	6000	psi	atm	$2,500.00
LOX Supply Tank	1	Praxair	1300	psi	90	$90.00
LCH4 Supply Tank	1	Praxair	1300	psi	111	$90.00
Load Cell	1	Interface Environment	5,000	lbf		$290.00
					TOTAL	**$18,465.92**

If GPI is able to sponsor the engine entirely, we will have adequate funds to pay for the additional test stand enhancements, facilitating a possible static test by the end of June.

8.0 CONCLUSIONS

After the hydro flow test of the first iteration of the Leon 1, it appears that both design and manufacturing of the engine have been completed properly. The second iteration of the engine is expected to be delivered within the coming days and will be hydro tested immediately in order to

prepare for a static fire of the Cobalt Chromium version. Before this can be done, however, further funds must be raised not only to pay for the 3D printing, but for the various items required to modify the test stand for use by SEDS SJSU. Even after the final presentations and degree requirements are completed, we will continue with this process until completion of the full project. We aim to make this project an annual or bi-annual effort for the organization, to not only further educate students in the areas of rocketry and propulsion, but to bring recognition to the department and the university.

RFERENCES

N. Willett, 'Water On Mars | Mars Society Education Forum',*Education2.marssociety.org*, 2015. [Online]. Available: http://education2.marssociety.org/category/curriculum/water-on-mars/.

Wikipedia, 'Wernher von Braun', 2015. [Online]. Available: http://en.wikipedia.org/wiki/Wernher_von_Braun.

Wikipedia, 'Gas-generator cycle', 2015. [Online]. Available: http://en.wikipedia.org/wiki/Gas-generator_cycle.

S. Sullivan and T. Hanks, *Virtual Apollo*. Ontario, Canada: Collector's Guide Pub., 2002.

Wikipedia, 'Apollo Lunar Module', 2015. [Online]. Available: http://en.wikipedia.org/wiki/Apollo_Lunar_Module.

'MSL Landing Special', 2015. [Online]. Available: http://www.spaceflight101.com/msl-landing-special.html

Hyperphysics.phy-astr.gsu.edu, 'Ideal Gas Law', 2015. [Online]. Available: http://hyperphysics.phy-astr.gsu.edu/hbase/kinetic/idegas.html.

En.citizendium.org, 'de Laval nozzle - encyclopedia article - Citizendium', 2015. [Online]. Available: http://en.citizendium.org/wiki/De_Laval_nozzle.

Wikipedia, 'Pressure-fed engine', 2015. [Online]. Available: http://en.wikipedia.org/wiki/Pressure-fed_engine.

Wikipedia, 'Energy density', 2015. [Online]. Available: http://en.wikipedia.org/wiki/Energy_density.

P. Hill and C. Peterson, *Mechanics and thermodynamics of propulsion*. Reading, Mass.: Addison-Wesley Pub. Co, 1965.

Wikipedia, 'Falcon 1', 2015. [Online]. Available: http://en.wikipedia.org/wiki/Falcon_1.

M. Dawson, G. Brewster, C. Conrad, M. Kilwine, B. Chenevert and O. Morgan, 'Monopropellant Hydrazine 700 lbf Throttling Terminal Descent Engine for Mars Science Laboratory', *43rd AIAA/ASME/SAE/ASEE Joint Propulsion Conference & Exhibit*, no. 5481, 2007.

Gpiprototype.com, 'DMLS - Direct Metal Laser Sintering | Services', 2015. [Online]. Available: http://gpiprototype.com/services/dmls-direct-metal-laser-sintering.html.

D. Huzel, D. Huang and H. Arbit, *Modern engineering for design of liquid-propellant rocket engines*. Washington, D.C.: American Institute of Aeronautics and Astronautics, 1992.

G. Sutton, *Rocket Propulsion Elements*. New York: Wiley, 1986.

R. Braeunig, 'Basics of Space Flight: Rocket Propulsion', *Braeunig.us*, 2015. [Online]. Available: http://www.braeunig.us/space/propuls.htm.

R. Braeunig, 'Propellant Combustion Charts', *Braeunig.us*, 2005. [Online]. Available: http://www.braeunig.us/space/comb.htm.

Wikipedia, 'Gibbs free energy', 2015. [Online]. Available: http://en.wikipedia.org/wiki/Gibbs_free_energy.

H. Föll, 'The chemical potential', *Tf.uni-kiel.de*. [Online]. Available: http://www.tf.uni-kiel.de/matwis/amat/def_en/kap_2/advanced/t2_4_1.html

A. Ponomarenko, *RPA: Tool for Liquid Propellant Rocket Engine Analysis C++ Implementation*. Rocket Propulsion Analysis, 2010.

S. Gordon and B. McBride, 'Computer Program for Calculation of Complex Chemical Equilibrium Compositions and Applications', National Aeronautics and Space Administration, Cleveland, OH, 1994.

Kinetics.nist.gov, 'NIST-JANAF Thermochemical Tables', 2013. [Online]. Available: http://kinetics.nist.gov/janaf/.

Material data sheet - EOS CobaltChrome MP1 for EOSINT M 270, 1st ed. Munich, Germany: GPI Protoype & Manufacturing, 2007, pp. 3 - 6.

Holthaus, M. *Design and Test: FAR-004*. Friends of Amateur Rocketry, Inc. 2010

Y. Cengel and A. Ghajar. Heat and Mass Transfer: *Fundamentals & Applications, Fifth Edition*. McGraw-Hill Education, 2015.

Design and Test

FAR-0004

Revision --

May 12, 2010

By: Mark Holthaus

Rocket Design Review Checklist	
1.	Vehicle stability analysis (Center-of-Gravity versus Center-of-Pressure)
2.	Fin attachment strength
3.	Structural strength
4.	Thrust structure strength.
5.	Launch lugs (Minimum 2)
6.	Launch lug strength
7.	Fuel tank hydrostatic test (>125% Operating Pressure)
8.	Oxidizer tank hydrostatic test (>125% Operating Pressure)
9.	Pressurization system tank analysis (>125% Operating Pressure)
10.	Altitude analysis
11.	Vehicle weight
12.	Vehicle dimensions
13.	Static firing test.
14.	Water flow test.
15.	Injector water flow test.
16.	Main valve open and close.
17.	Propellant tank remote controlled vents.
18.	Propellant tank pressure relief valves.
19.	Low-point, propellant tank fill and drain valves.
20.	Remote controlled pressurant fill quick disconnect.
21.	Remote controlled pressurant on and off valve.
22.	Propellant tank pressurization, check valves.
23.	Propellant tank pressurization diffuses.
24.	Material and propellant compatibility evaluation.
25.	Components cleaned for propellant.
26.	Pressure transducers on propellant tanks.

Rocket Design Review Checklist	
27.	Pressure transducer on pressurant tank.
28.	Develop countdown sequence.
29.	Develop abort sequence.
30.	Develop prelaunch procedures.
31.	Develop abort procedures.

Rocket Static Firing Design Review Checklist	
1.	Mounting structural strength
2.	Rocket motor mounting strength.
3.	Fuel tank hydrostatic test (>125% Operating Pressure)
4.	Oxidizer tank hydrostatic test (>125% Operating Pressure)
5.	Pressurization system tank analysis (>125% Operating Pressure)
6.	Injector water flow test.
7.	Water flow test.
8.	Remote controlled main valve open and close.
9.	Propellant tank remote controlled vents.
10.	Propellant tank pressure relief valves.
11.	Low-point propellant tank fill and drain valve.
12.	Remote control pressurant on and off valve.
13.	Propellant tank pressurization check valve.
14.	Propellant tank pressurization diffuser.
15.	Material and propellant compatibility evaluation.
16.	Components cleaned for propellant.
17.	Pressure transducers on propellant tanks.
18.	Pressure transducer on pressurant tank.
19.	Load cell on rocket motor.
20.	Pressure transducer on combustion chamber.
21.	Develop countdown sequence.
22.	Develop abort sequence.
23.	Develop pretest procedures.
24.	Develop abort procedures.

	Ground Support Equipment Design Review Checklist
1.	Electrical Controls ☐ Main Valve Open and Close ☐ Fuel Vent Open and Close ☐ Oxidizer Vent Open and Close ☐ Pressurant On and Off ☐ Umbilical Release ☐ High-Pressure Control Valve ☐ Igniter Initiate
2.	Computer Control ☐ Computer ☐ Monitor ☐ Keyboard ☐ Mouse
	☐ Interface
3.	Software ☐ Launch sequencing ☐ Abort sequencing ☐ Checkout sequencing ☐ Parameter display ☐ Warnings and alarms ☐ Data archival
4.	Electrical Umbilical
5.	Electrical Extension ☐ 1000-Foot Cable ☐ Cable Reel
6.	Data Acquisition ☐ Rocket Sensors (Pressure, Temperature, Valve Position) ☐ Pad Sensors (Pressure, Valve Position) ☐ Acquisition Unit ☐ Computer with Monitor and Keyboard
7.	Emergency Manual Control ☐ Main Valve Close ☐ Fuel Vent Open ☐ Oxidizer Vent Open ☐ Pressurant Off

	Ground Support Equipment Design Review Checklist
8.	Fuel Loading • Tank/Dewar • Loading Hose • Hose Wrench
9.	Oxidizer Loading • Tank/Dewar • Loading Hose • Hose Wrench
10.	Pressurant Loading • Remote Control High-Pressure Valve • High-Pressure Hose • High-Pressure Bottle • Pressurant Umbilical with Remote Control Quick Disconnect
11.	Pneumatic Pressurant • Low-Pressure Regulator • Low-Pressure Hose • Pressure Bottle
12.	Launch Rail • Support Tower • Tower Base • Rail Guide • Rocket Support Bracket
13.	Flame Deflector
14.	Launch Pad Power
15.	Electrical Control Power
16.	Control software • Countdown sequence • Abort sequence • Checkout sequence

Tank Hydrostatic Test Procedure	
1.	Check the tank for dents and damage. If the tank is dented or damaged, do not do this test.
2.	WARNING: HIGH-PRESSURE OPERATIONS. Wear safety glasses. Limit people handling and standing near the tank when pressurized.
3.	Completely fill tank with water. WARNING: Do not leave any air pockets in the tank. Fill from the bottom of the tank and vent the air from the top.
4.	Check and tighten all fittings to make sure they are not leaking.
5.	Using a water hand pump, pump the tank pressure up to 150% of the operating pressure. WARNING: If the tank pressure is not rising while pumping, the tank is expanding and may rupture. STOP PUMPING.
6.	Hold the pressure for 3-minutes.
7.	Relieve the pressure.
8.	Pressurize and relieve the tank two additional times using steps 4 through 6.
9.	If the tank bursts, springs a leak, or deforms: the tank is unusable.
10.	Drain the tank of water.
11.	Rinse the tank with isopropyl alcohol.
12.	Force air through the tank to dry out.
13.	When you can do longer smell alcohol in the tank, it is dry.

	Water Flow Test Procedure
1.	Calculate fuel and oxidizer volume flow rate for the rocket engine.
2.	Calculate the flow duration based on propellant tank volumes and the propellant volume flow rate.
3.	Calculate fuel and oxidizer orifice size with equivalent water volume flow. Please Note: When using water with full feed pressure drop to the atmosphere across the orifice, the water will cavitate in the orifice. Utilize a C_d of 0.611 for a cavitating orifice.
4.	Machine water flow test fuel and oxidizer feedline orifices.
5.	Setup test stand.
6.	Setup data acquisition system to record fuel, oxidizer, and pressurant tank pressures.
7.	Remove rocket motor.
8.	Install orifices in place of the injector.
9.	Perform rocket leak test.
10.	Perform rocket valve test.
11.	Mount the rocket in the test stand.
12.	Load pressurant.
13.	Load water into propellant tanks.
14.	Start data acquisition system.
15.	Perform 3-second countdown.
16.	On 0-count open main valves.
17.	Stop the data acquisition when all the water runs out.
18.	From the recorded data, time the water flow from main valve open until the water runs out.
19.	Compare the water flow duration to the calculated flow duration.
20.	From the recorded data, check the pressure regulator output pressure to see if the regulator is supplying the

	Water Flow Test Procedure
	expected pressure. If the pressure drops too low, the regulator is not keeping up with the expected flow rate.
21.	Dismount rocket from test stand.
22.	Remove main ball valves from the rocket.
23.	CAUTION: FOR CRYOGENIC PROPELLANTS. Take apart the ball valves and thoroughly dry all internal parts. Water on the inside of the ball valve can freeze solid when using cryogenic propellants and cause a hang fire.

Injector Water Flow Test Procedure	
1.	Calculate fuel and oxidizer volume flow rate for the rocket engine.
2.	Calculate the equivalent water weight
3.	Connect a water source to the fuel side of the injector.
4.	Start the water flowing. Adjust the flow rate until in input pressure is 20-psig.
5.	Spray and collect the water into a bucket for 5-minutes.
6.	Weigh the amount of water.
7.	Perform steps 2 through 4 for two more times.
8.	Calculate an average orifice size.
9.	Connect a water source to the oxidizer side of the injector.
10.	Start the water flowing. Adjust the flow rate until in input pressure is 20-psig.
11.	Spray and collect the water into a bucket.
12.	Time the water until the bucket is full.
13.	Record the time and input pressure.
14.	Weigh the amount of water.
15.	Record the water weight.
16.	Perform steps 8 through 10 for two more times.
17.	Connect water to both the oxidizer and fuel sides of the injector.
18.	Visually check the impingement pattern from the injector holes. Water streams emanating from the fuel and oxidizer orifice pairs should impinge at expected angles.
19.	Dry the injector.
20.	Calculate water mass flowrate for each measurement.
21.	Calculate the C_d for the orifices based on the number of injector holes, injector hole size, water flow test feed pressure, and water mass flow rate. The resulting C_d for the orifices should be approximately 0.8.

Injector Water Flow Test Procedure	
22.	Adjust orifices size and angle if the results are not what are expected and redo water flow testing.
23.	

	Rocket Valve Test Procedure
1.	Setup electrical ground support equipment.
2.	Setup mechanical ground support equipment.
3.	Connect the electrical umbilical between the electrical ground support equipment and the rocket.
4.	Connect the pressurant umbilical between the mechanical ground support equipment and the rocket.
5.	Place all switches in the closed position.
6.	Turn on the pneumatic pressure to 100-psi.
7.	Turn the electrical ground support equipment power on.
8.	Command main valve open.
9.	Command main valve closed.
10.	Command fuel tank vent open.
11.	Command fuel tank vent closed.
12.	Command oxidizer tank vent open.
13.	Command oxidizer tank vent closed.
14.	Command pressurization valve open.
15.	Command pressurization valve closed.
16.	Command pre-pressurization valve open.
17.	Command pre-pressurization valve closed.
18.	Command umbilical to disconnect.

	Leak Test Procedure
1.	To start the leak test insure the main valve is closed.
2.	Verify the helium pressurization system is at ambient pressure.
3.	**WARNING: HIGH-PRESSURE**. Have a minimum crew near the tanks and wear safety glasses when tanks are pressurized. Always work in teams of two.
	Oxidizer tank pressure decay test.
4.	Connect a low-pressure helium pressurizer to the oxidizer fill and drain port.
5.	Open the oxidizer fill and drain valve.
6.	Pressurize the oxidizer tank to 100-psi.
7.	Close the oxidizer fill and drain valve.
8.	Relieve the pressure on the helium source line.
9.	Monitor oxidizer tank pressure. If the pressure decreases by more than 1-psi in 5-minutes, there is a leak that needs to be fixed. Perform a bubble test on oxidizer fittings and valves.
10.	Monitor the pressurant system pressure. If the pressure increases by more than 1-psi in 5-minutes, there is a leak in the oxidizer tank pressurant check valve.
11.	If the leak test is successful, leave the oxidizer tank pressurized.
12.	Disconnect the low-pressure helium pressurizer from the oxidizer fill and drain port.
	Fuel tank pressure decay test.
13.	Connect a low-pressure helium pressurizer to the fuel fill and drain port.
14.	Open the fuel fill and drain valve.
15.	Pressurize the fuel tank to 100-psi.
16.	Close the fuel fill and drain valve.
17.	Relieve the pressure on the helium source line.

	Leak Test Procedure
18.	Monitor fuel tank pressure. If the pressure decreases at more than 1-psi for 5-minutes, there is a leak that needs to be fixed. Perform a bubble test on fuel fittings and valves.
19.	Monitor the pressurant system pressure. If the pressure increases by more than 1-psi in 5-minutes, there is a leak in the fuel tank pressurant check valve.
20.	If the leak test is successful, leave the fuel tank pressurized.
21.	Disconnect the low-pressure helium pressurizer from the fuel fill and drain port.
	Pressurant system pressure decay test.
22.	Connect a low-pressure helium pressurizer to the pressurant fill and drain port.
23.	Open the pressurant fill and drain valve.
24.	Pressurize the pressurant tank to 100-psi.
25.	Close the pressurant fill and drain valve.
26.	Relieve the pressure on the helium source line.
27.	Monitor fuel pressurant pressure. If the pressure decreases at more than 1-psi for 5-minutes, there is a leak that needs to be fixed. Perform a bubble test on pressurant fittings and valves.
28.	Open the pressurant fill and drain valve to relieve the pressurant tank pressure.
29.	Close the pressurant fill and drain valve.
30.	Open the oxidizer fill and drain valve to relieve the oxidizer tank pressure.
31.	Close the oxidizer fill and drain valve.
32.	Open the fuel fill and drain valve to relieve the fuel tank pressure.
33.	Close the fuel fill and drain valve.
	Rocket motor pressure decay test.
34.	Clamp a plug on the exit of the rocket nozzle.

	Leak Test Procedure
35.	Connect a low-pressure helium pressurizer to the rocket motor plug valve.
36.	Open the plug valve and pressurize the rocket motor to 100-psi.
37.	Close the plug valve.
38.	Relieve the pressure on the helium source line.
39.	Monitor the rocket motor pressure. If the pressure decreases at more than 1-psi for 5-minutes, there is a leak that needs to be fixed. Perform a bubble test on fittings and valves.
40.	Open the plug valve to relieve the rocket motor pressure.
41.	Remove the rocket nozzle plug.
	End of Leak Test
	Bubble Soap Test
1.	If the pressure decay test fails, perform the following:
2.	Prepare a 5% soap and water solution in a spray or squirt bottle.
3.	With plumbing pressurized perform the following steps.
4.	Spray soap solution on tube and pipe joints.
5.	Spray soap solution on fitting joints.
6.	Spray soap solution on valve joints.
7.	Spray soap solution on valve body joints and stems.
8.	Spray soap solution on manifold joints.
9.	Spray soap solution on tank joints.
10.	Look for bubbles forming. If bubbles are forming, tighten the joint. If the bubbles persist, re-connect the joint using new pipe tape, conical seals, or O-rings. If the bubbles are forming on a valve body seams, replace the valve.
11.	Spray soap solution on your finger and wipe over the output ports of the following:

	Leak Test Procedure
12.	Wipe the fill and drain valve output.
13.	Wipe the relief valve output.
14.	Wipe the manual vent-valve output.
15.	Wipe the remote control vent-valve output.
16.	Look for bubbles forming at the valve output. If bubbles are forming, replace the valve.
17.	If the rocket motor is pressurized, spray soap solution on rocket motor joints.
18.	Look for bubbles forming. If bubbles are forming, replace rocket motor body O-rings.

	Rocket Static Test Preparation Procedure
1.	Fuel tank low pressure, pressure decay test.
2.	Oxidizer tank low pressure, pressure decay test.
3.	Main valve open and close test.
4.	Fuel tank vent command open and close test.
5.	Oxidizer tank vent command open and close test.
6.	Pressurization valve command open and close test.
7.	Pressurization system low pressure, pressure decay test.
8.	Pre-pressurization valve command open and close test.
9.	Inspect catalyst.
10.	Load reloads.
11.	Install nozzle.
12.	**CAUTION:** Make sure all seals are in place and all closures are firmly in place.
13.	Calibrate load cell.
14.	Verify pressure transducer function.

13 Check list

1 Part geometry	
Get only the moulding structures built?	
Are the exterior dimensions as small as possible?	
Wall thickness for cavities: 10 mm (5mm for DirectSteel H20)	
Inserts should have round corners (e. g. Fig. 2) Radius 10 or 20mm	
Is the building platform (thickness: 22mm or 36mm) to be used as part of the tool?	
2 Drill holes	
Are all drill holes designed into the CAD file?	
Ejector drill holes	
Gating system drill holes	
Threaded holes designed as simple holes (1mm smaller than destined diameter)	
Diameter of drill holes in CAD file 0.6 mm smaller than destined diameter	
4 Minimum structures	
Can sharp edges and corners be avoided?	
Are the structures smaller than 0.6 mm?	
5 Slots	
Are there draft angles for deep slots?	
Are the slots well accessible for grinding and polishing?	
Does the tool have to be split?	
6 Ribs	
Should steel ribs be inserted?	
Are the pockets required for this provided in the CAD data?	
7 Pins	
Plan cylindrical pins as inserts!	
Should non-cylindrical pins be planned as inserts?	
8 Gating channel	
Is there already a gating channel in the CAD file?	
9 Cooling channels	
Can 3-dimensionally laid cooling channels be used?	
Are these close to the modelling geometry?	
Can the building time be kept to a minimum?	
10 Operational overmeasures	
Has machining allowance been added for the fitting of the inserts into the mother tool?	
Has machining allowance been added to the parting planes?	
11 Mounting into mother tool	
Are the inserts mounted comprehensively?	
Does the locking pressure rest on the mother tool as well or only on the inserts?	
12 Data quality	
Do all planes intersect?	
Have all double planes been removed?	
Is the mesh density set to a suitable value for the STL generation (e. g. 0.02mm for DirectSteel 20 or 0.05 for DirectMetal 50)?	

APPENDIX C: RPA Applied Heating Outputs without Cooling Design

Location (in)	Radius (in)	Conv. Heat Coeff. (Btu/in^2-s-^{o}R)	Conv. Heat Flux (Btu/in^2-s)	Rad. Heat Flux (Btu/in^2-s)	Total Heat (Btu/in^2-s)	T_{wg} (^{o}R)	T_{wi} (^{o}R)	T_{we} (^{o}R)
0.000	2.126	0.0009	1.1437	0.2194	1.3631	4,728.95	4,728.95	4,694.05
0.246	2.126	0.0009	1.0538	0.4100	1.4639	4,825.95	4,825.95	4,778.50
0.492	2.126	0.0009	1.0538	0.4100	1.4639	4,825.95	4,825.95	4,778.50
0.739	2.126	0.0009	1.0538	0.4100	1.4639	4,825.95	4,825.95	4,778.50
0.946	2.126	0.0009	1.0544	0.4085	1.4630	4,825.26	4,825.26	4,777.78
1.069	2.124	0.0009	1.0522	0.4144	1.4666	4,829.35	4,829.35	4,780.76
1.193	2.119	0.0009	1.0585	0.4101	1.4685	4,828.36	4,828.36	4,782.32
1.316	2.109	0.0009	1.0607	0.4124	1.4731	4,834.69	4,834.69	4,786.05
1.439	2.096	0.0009	1.0682	0.4124	1.4807	4,839.58	4,839.58	4,792.16
1.562	2.079	0.0009	1.0761	0.4095	1.4856	4,847.25	4,847.25	4,796.15
1.685	2.059	0.0009	1.0887	0.4027	1.4913	4,854.11	4,854.11	4,800.75
1.808	2.034	0.0009	1.0999	0.4075	1.5074	4,866.94	4,866.94	4,813.66
1.931	2.006	0.0009	1.1176	0.3987	1.5163	4,877.02	4,877.02	4,820.73
2.054	1.973	0.0010	1.1372	0.3950	1.5322	4,890.34	4,890.34	4,833.32
2.177	1.937	0.0010	1.1581	0.3873	1.5454	4,906.54	4,906.54	4,843.72
2.301	1.896	0.0010	1.1846	0.3791	1.5638	4,923.33	4,923.33	4,858.02
2.424	1.851	0.0011	1.2133	0.3761	1.5894	4,944.14	4,944.14	4,877.82
2.547	1.801	0.0011	1.2436	0.3706	1.6142	4,968.98	4,968.98	4,896.72
2.670	1.746	0.0012	1.2800	0.3643	1.6443	4,995.64	4,995.64	4,919.42
2.793	1.687	0.0013	1.3219	0.3494	1.6713	5,024.60	5,024.60	4,939.47
2.916	1.622	0.0014	1.3695	0.3441	1.7136	5,058.30	5,058.30	4,970.45
3.039	1.552	0.0015	1.4226	0.3292	1.7518	5,095.84	5,095.84	4,997.91
3.162	1.475	0.0016	1.4889	0.3071	1.7960	5,135.17	5,135.17	5,029.16
3.285	1.393	0.0018	1.5608	0.2926	1.8533	5,182.46	5,182.46	5,068.81
3.409	1.304	0.0020	1.6401	0.2811	1.9212	5,237.39	5,237.39	5,114.59
3.532	1.208	0.0023	1.7392	0.2559	1.9950	5,296.00	5,296.00	5,163.02
3.655	1.105	0.0027	1.8521	0.2258	2.0779	5,361.55	5,361.55	5,215.83
3.778	1.002	0.0032	1.9720	0.2047	2.1767	5,431.54	5,431.54	5,276.73
3.901	0.899	0.0038	2.1056	0.1684	2.2740	5,501.24	5,501.24	5,334.76
4.024	0.800	0.0047	2.2360	0.1375	2.3735	5,569.11	5,569.11	5,392.19
4.147	0.726	0.0055	2.3465	0.1034	2.4499	5,614.85	5,614.85	5,435.06
4.270	0.675	0.0062	2.4199	0.0691	2.4891	5,640.66	5,640.66	5,456.66
4.393	0.643	0.0067	2.4589	0.0368	2.4957	5,648.27	5,648.27	5,460.27
4.517	0.628	0.0070	2.4704	0.0185	2.4890	5,639.14	5,639.14	5,456.61
4.567	0.627	0.0070	2.4636	0.0118	2.4754	5,630.66	5,630.66	5,449.14
4.814	0.702	0.0054	2.2703	-0.0284	2.2419	5,479.84	5,479.84	5,315.85
5.060	0.792	0.0042	2.0939	-0.0283	2.0656	5,360.13	5,360.13	5,208.10

5.306	0.879	0.0035	1.9504	-0.0273	1.9231	5,254.64	5,254.64	5,115.85
5.552	0.965	0.0029	1.8258	-0.0280	1.7978	5,158.27	5,158.27	5,030.41
5.798	1.049	0.0024	1.7169	-0.0272	1.6898	5,069.02	5,069.02	4,953.06
6.045	1.131	0.0021	1.6194	-0.0272	1.5922	4,985.79	4,985.79	4,879.97
6.291	1.211	0.0019	1.5331	-0.0263	1.5068	4,907.66	4,907.66	4,813.19
6.537	1.289	0.0016	1.4544	-0.0247	1.4297	4,834.60	4,834.60	4,750.36
6.783	1.366	0.0015	1.3837	-0.0246	1.3591	4,765.43	4,765.43	4,690.63
7.030	1.441	0.0013	1.3191	-0.0233	1.2958	4,700.48	4,700.48	4,635.01
7.276	1.514	0.0012	1.2599	-0.0227	1.2373	4,639.14	4,639.14	4,581.77
7.522	1.586	0.0011	1.2058	-0.0215	1.1842	4,581.24	4,581.24	4,531.85
7.768	1.657	0.0010	1.1560	-0.0206	1.1354	4,526.43	4,526.43	4,484.42
8.015	1.726	0.0009	1.1101	-0.0199	1.0903	4,474.51	4,474.51	4,439.14
8.261	1.794	0.0009	1.0676	-0.0190	1.0486	4,425.45	4,425.45	4,396.11
8.690	1.908	0.0008	1.0008	-0.0182	0.9826	4,345.52	4,345.52	4,325.23

APPENDIX D: RPA Heating Outputs with Cooling Design

Location (in)	Radius (in)	Conv. Heat Coeff. (Btu/in²-s-°R)	Conv. Heat Flux (Btu/in²-s)	Rad. Heat Flux (Btu/in²-s)	Total Heat (Btu/in²-s)	T_{wg} (°R)	T_{wi} (°R)	T_{wc} (°R)	T_c (°R)
0.000	2.126	0.0000	0.0000	0.5833	0.5833	437.61	437.61	376.11	330.20
0.246	2.126	0.0000	0.0000	0.7756	0.7756	471.59	471.59	390.54	329.10
0.492	2.126	0.0000	0.2246	0.7579	0.9825	506.69	506.69	406.05	327.67
0.739	2.126	0.0002	1.1162	0.7059	1.8221	659.61	659.61	473.60	325.34
0.946	2.126	0.0003	1.4387	0.6846	2.1233	713.82	713.82	497.16	322.51
1.069	2.124	0.0003	1.5856	0.6757	2.2613	739.26	739.26	508.59	320.63
1.193	2.119	0.0003	1.6489	0.6635	2.3124	750.66	750.66	514.78	318.64
1.316	2.109	0.0003	1.6756	0.6633	2.3389	759.59	759.59	520.94	316.60
1.439	2.096	0.0003	1.6912	0.6605	2.3517	767.69	767.69	527.75	314.53
1.562	2.079	0.0003	1.7039	0.6597	2.3635	777.18	777.18	536.06	312.44
1.685	2.059	0.0003	1.7187	0.6560	2.3747	787.79	787.79	545.55	310.32
1.808	2.034	0.0003	1.7358	0.6572	2.3930	800.67	800.67	556.59	308.17
1.931	2.006	0.0003	1.7583	0.6543	2.4126	814.24	814.24	568.13	306.00
2.054	1.973	0.0003	1.7872	0.6505	2.4377	828.48	828.48	579.88	303.81
2.177	1.937	0.0003	1.8221	0.6502	2.4723	843.96	843.96	591.85	301.59
2.301	1.896	0.0004	1.8666	0.6458	2.5125	859.03	859.03	602.79	299.34
2.424	1.851	0.0004	1.9217	0.6439	2.5657	874.27	874.27	612.66	297.06
2.547	1.801	0.0004	1.9900	0.6445	2.6345	889.13	889.13	620.55	294.74
2.670	1.746	0.0004	2.0731	0.6431	2.7162	904.07	904.07	627.17	292.37
2.793	1.687	0.0004	2.1722	0.6412	2.8134	920.00	920.00	633.10	289.95
2.916	1.622	0.0004	2.2919	0.6396	2.9315	936.98	936.98	638.09	287.46
3.039	1.552	0.0005	2.4372	0.6386	3.0758	955.12	955.12	641.58	284.89
3.162	1.475	0.0005	2.6183	0.6316	3.2499	973.49	973.49	642.19	282.25
3.285	1.393	0.0006	2.8429	0.6296	3.4724	993.61	993.61	639.52	279.51
3.409	1.304	0.0006	3.1306	0.6299	3.7605	1,014.76	1,014.76	631.34	276.65
3.532	1.208	0.0007	3.5150	0.6237	4.1387	1,035.21	1,035.21	613.22	273.63
3.543	1.199	0.0007	3.5582	0.6230	4.1813	1,037.06	1,037.06	610.79	273.34
3.543	1.199	0.0008	4.0451	0.6349	4.6800	912.13	912.13	434.97	273.34
3.655	1.105	0.0008	3.8866	0.6146	4.5011	1,088.78	1,088.78	629.84	270.34
3.778	1.002	0.0008	4.0050	0.6021	4.6071	1,211.59	1,211.59	741.88	267.29
3.901	0.899	0.0009	4.3766	0.5854	4.9620	1,292.18	1,292.18	786.27	264.40
4.024	0.800	0.0010	4.8939	0.5645	5.4584	1,359.63	1,359.63	803.08	261.66
4.147	0.726	0.0012	5.4120	0.5282	5.9402	1,405.03	1,405.03	799.31	259.16
4.270	0.675	0.0013	5.8586	0.4903	6.3489	1,433.54	1,433.54	786.09	256.86
4.393	0.643	0.0014	6.1918	0.4435	6.6353	1,447.85	1,447.85	771.07	254.66
4.517	0.628	0.0014	6.3651	0.3969	6.7620	1,450.09	1,450.09	760.32	252.52
4.567	0.627	0.0014	6.3812	0.3814	6.7626	1,447.95	1,447.95	758.14	251.65

4.814	0.702	0.0013	5.6784	0.1655	5.8439	1,361.41	1,361.41	765.55	247.38
5.060	0.792	0.0011	5.0067	0.1057	5.1125	1,278.85	1,278.85	757.62	242.99
5.306	0.879	0.0010	4.5028	0.0814	4.5842	1,200.32	1,200.32	732.93	238.63
5.552	0.965	0.0009	4.1224	0.0673	4.1897	1,122.40	1,122.40	695.23	234.27
5.798	1.049	0.0008	3.8896	0.0575	3.9470	1,030.56	1,030.56	628.14	229.84
6.045	1.131	0.0008	3.8178	0.0503	3.8681	910.39	910.39	516.01	225.22
6.291	1.211	0.0008	3.9452	0.0448	3.9901	741.48	741.48	334.65	220.22
6.299	1.213	0.0008	3.9547	0.0448	3.9994	734.42	734.42	326.63	220.04
6.299	1.213	0.0007	3.4291	0.0437	3.4728	879.87	879.87	525.80	220.04
6.537	1.289	0.0006	3.1279	0.0393	3.1671	853.46	853.46	530.55	215.67
6.783	1.366	0.0006	2.8689	0.0349	2.9038	826.72	826.72	530.65	211.26
7.030	1.441	0.0005	2.6520	0.0314	2.6834	800.36	800.36	526.76	206.98
7.276	1.514	0.0005	2.4680	0.0287	2.4966	774.47	774.47	519.91	202.78
7.522	1.586	0.0005	2.3103	0.0263	2.3366	749.00	749.00	510.75	198.67
7.768	1.657	0.0004	2.1723	0.0241	2.1964	724.84	724.84	500.87	194.63
8.015	1.726	0.0004	2.0520	0.0223	2.0743	701.08	701.08	489.55	190.66
8.261	1.794	0.0004	1.9469	0.0209	1.9678	677.48	677.48	476.80	186.74
8.690	1.908	0.0004	1.8000	0.0186	1.8186	632.37	632.37	446.86	180.00

APPENDIX E: Matlab Code for Thermal Equilibrium Analysis (with assistance from Armani Batista)

```matlab
% Loop Unrolled Calculation of Change in Enthalpy compared to Heat of
% Reaction, with mole fractions and Tc as Variables.
% 5/3/15
% Version 1.1
%
% Notes:
%       1. Use n(11-13), using n_ gb(11-13) instead. Also n_gb(14)
%          gives better results
%


clear
%clc

ROWS = 41;
NG = 14;
COLS = NG;

p = zeros(ROWS,1);
for i=0:ROWS-1
    p(i+1) = i;
end

%    Coefficients
%H2O c1=[-
9.908783887
0.033143752
-1.00206E-06
3.68542E-09
2.45728E-12
-3.87537E-15
1.86712E-18
-3.75223E-22
-7.98313E-27
1.37955E-29
6.2276E-34
-9.21409E-37
5.22734E-41
2.91346E-44
-2.96287E-48
-3.8216E-52
9.17278E-57
5.92693E-60
1.30969E-63
-2.78545E-67
2.15891E-71
-2.38909E-75
1.09487E-78
-6.80646E-83
-6.71141E-86
5.91714E-90
-1.32349E-93
5.68484E-97
1.3427E-102
```

104

```
-7.9127E-105
9.9023E-109
-2.5642E-112
-3.5815E-116
9.8299E-120
-8.3773E-124
1.3923E-127
4.4222E-131
-9.7704E-135
-5.4586E-139
1.7709E-142
-7.6556E-147
];

%CO
c2 = [-8.676693377
0.029332213
-1.3888E-06
1.17505E-10
8.22407E-12
-9.93056E-15
5.11548E-18
-1.12811E-21
-2.86029E-26
5.16332E-29
-1.20104E-34
-2.77837E-36
1.86779E-40
8.07766E-44
-7.78254E-48
-9.63611E-52
-1.99985E-56
1.66628E-59
3.99269E-63
-6.31472E-67
2.47769E-71
-6.01226E-75
2.50815E-78
-5.8261E-84
-1.58395E-85
1.07629E-89
-3.79307E-93
1.66655E-96
-2.8E-101
-2.1369E-104
3.0814E-108
-7.2302E-112
-1.0602E-115
3.3972E-119
-2.83E-123
3.3219E-127
1.1583E-130
-2.6183E-134
-1.769E-138
5.844E-142
-2.8251E-146
];

% H2
```

```
c3 = [-8.567168545
0.037651393
-7.52518E-05
2.41207E-07
-3.93936E-10
3.70794E-13
-2.08837E-16
6.79315E-20
-9.83484E-24
-9.20754E-28
5.91881E-31
-7.26994E-35
-3.56828E-39
1.82217E-42
-1.80752E-46
8.37463E-51
-6.01286E-54
2.39881E-57
-1.53051E-61
-7.94769E-65
1.51084E-68
-1.34422E-72
2.28458E-76
2.79022E-80
-1.38962E-83
4.23531E-88
7.1481E-92
-1.91206E-95
5.7091E-99
-3.1337E-103
1.6573E-106
-2.4334E-110
-6.6047E-115
-1.7031E-118
-1.3449E-121
2.2812E-125
4.2517E-129
-6.6754E-133
6.5623E-137
-1.5994E-140
1. 2044E-144
];

% CO2
c4 = [-9.336602376
0.027073513
6.52997E-06
4.38066E-08
-6.99373E-11
5.31327E-14
-2.20453E-17
4.19397E-21
1.76531E-25
-1.8559E-28
-5.28456E-33
1.12149E-35
-6.78513E-40
-3.32634E-43
3.27773E-47
```

```
3.99771E-51
7.00228E-57
-6.18882E-59
-1.63856E-62
2.88474E-66
-1.86918E-70
2.54149E-74
-1.14815E-77
4.65794E-82
7.37623E-85
-6.06235E-89
1.56493E-92
-6.72552E-96
3.9486E-101
8.9908E-104
-1.2304E-107
3.0817E-111
4.3206E-115
-1.2905E-118
1.0538E-122
-1.4276E-126
-5.0897E-130
1.1173E-133
6.8975E-138
-2.2429E-141
1. 0268E-145
];

% OH
c5 = [-9.116485551
0.026365923
3.87239E-05
-1.31412E-07
2.16324E-10
-2.01434E-13
1.12255E-16
-3.62424E-20
5.21508E-24
4.95385E-28
-3.16294E-31
3.89864E-35
1.8963E-39
-9.7747E-43
9.66287E-47
-4.4809E-51
3.22349E-54
-1.27891E-57
8.12408E-62
4.24769E-65
-8.07291E-69
7.17961E-73
-1.21336E-76
-1.51043E-80
7.41474E-84
-2.22875E-88
-3.82032E-92
1.02801E-95
-3.0407E-99
1.6524E-103
```

```
-8.8567E-107
1.2938E-110
3.5515E-115
9.0963E-119
7.1817E-122
-1.2153E-125
-2.2634E-129
3.5586E-133
-3.5248E-137
8.5492E-141
-6.4201E-145
];

% H
c6 = [-6.197041078
0.02077945
3.45942E-08
-8.22703E-11
1.03809E-13
-7.42958E-17
3.00831E-20
-6.10515E-24
1.97755E-28
1.74519E-31
-4.96425E-35
9.01447E-39
1.90149E-44
-3.89494E-46
2.76813E-50
4.84497E-54
9.24061E-58
-2.72838E-61
-7.74722E-66
9.48375E-69
-1.97309E-72
1.71446E-76
-1.60178E-80
-4.27547E-84
1.70682E-87
-2.77811E-92
-4.78442E- 96
2.843E-99
-8.0991E-103
-6.5313E-108
-2.0154E-110
2.3187E-114
1.1389E-119
4.9305E-122
2.1664E-125
-2.6766E-129
-4.7679E-133
8.3114E-137
-1.5517E-140
2.2048E-144
-9.4496E-149
];

% O2
c7 = [-8.701692596
```

```
0.030557657
-1.27779E-05
3.85239E-08
-4.81729E-11
3.63733E-14
-1.75097E-17
5.12712E-21
-6.80148E-25
-7.7497E-29
4.55834E-32
-5.84296E-36
-2.53857E-40
1.46532E-43
-1.40126E-47
6.91805E-52
-4.85762E-55
1.78807E-58
-1.08079E-62
-6.09038E-66
1.15546E-69
-1.0117E-73
1.57822E-77
2.5207E-81
-1.03994E-84
2.54206E-89
5.46219E-93
-1.554E-96
4.1248E-100
-1.9608E-104
1.2595E-107
-1.704E-111
-5.6719E-116
-1.2822E-119
-1.0222E-122
1.6746E-126
3.0719E-130
-4.8839E-134
5.2654E-138
-1.2159E-141
8. 8411E-146
];

% O
c8 = [-6.669892456
0.018078241
3.87297E-05
-1.29747E-07
2.12944E-10
-1.99665E-13
1.12031E-16
-3.63489E-20
5.25208E-24
4.93992E-28
-3.1688E-31
3.89658E-35
1.90706E-39
-9.76631E-43
9.67741E-47
-4.48987E-51
```

```
3.22254E-54
-1.28321E-57
8.17662E-62
4.25477E-65
-8.0876E-69
7.19435E-73
-1.22043E-76
-1.50012E-80
7.43519E-84
-2.25573E-88
-3.8271E-92
1.02544E-95
-3.0526E-99
1.6703E-103
-8.8712E-107
1.3005E-110
3.5444E-115
9.1118E-119
7.1975E-122
-1.22E-125
-2.2731E-129
3.5704E-133
-3.518E-137
8.562E-141
-6.4421E-145
];

% HCO
c9 = [-10.02672425
0.036281875
-2.7336E-05
8.92821E-08
-1.18456E-10
9.57276E-14
-4.90912E-17
1.51187E-20
-2.10324E-24
-2.16345E-28
1.33452E-31
-1.67382E-35
-7.79346E-40
4.19367E-43
-4.0878E-47
1.98999E-51
-1.38751E-54
5.32151E-58
-3.30927E-62
-1.78894E-65
3.39147E-69
-2.99713E-73
4.89426E-77
6.85156E-81
-3.08924E-84
8.46348E-89
1.61119E-92
-4.43799E-96
1.2457E-99
-6.3628E-104
3.7174E-107
```

```
-5.2579E-111
-1.5732E-115
-3.7885E-119
-3.0118E-122
5.0258E-126
9.2968E-130
-1.4673E-133
1.5064E-137
-3.5819E-141
2. 6545E-145
];

% HO2
c10 = [-10.14089664
0.042956221
-8.31275E-05
2.74332E-07
-4.25454E-10
3.84667E-13
-2.11041E-16
6.75062E-20
-9.63953E-24
-9.31049E-28
5.89062E-31
-7.2835E-35
-3.49924E-39
1.82553E-42
-1.80065E-46
8.40242E-51
-6.03614E-54
2.37564E-57
-1.5043E-61
-7.89606E-65
1.5019E-68
-1.33139E-72
2.23255E-76
2.84637E-80
-1.37606E-83
4.07348E-88
7.08949E-92
-1.91263E-95
5.6239E-99
-3.0341E-103
1.643E-106
-2.3805E-110
-6.7085E-115
-1.688E-118
-1.3356E-121
2.2527E-125
4.1858E-129
-6.5827E-133
6.5664E-137
-1.5869E-140
1. 1885E-144
];

% COOH
c11 = [0.00E+00
0.00E+00
```

```
0.00E+00
0.00E+00
0.00E+00
0.00E+00
0.00E+00
0.00E+00
0.00E+00
0.00E+00
0.00E+00
0.00E+00
0.00E+00
0.00E+00
0.00E+00
0.00E+00
0.00E+00
0.00E+00
0.00E+00
0.00E+00
0.00E+00
0.00E+00
0.00E+00
0.00E+00
0.00E+00
0.00E+00
0.00E+00
0.00E+00
0.00E+00
0.00E+00
0.00E+00
0.00E+00
0.00E+00
0.00E+00
0.00E+00
0.00E+00
0.00E+00
0.00E+00
0. 00E+00
];

% H2O2
%c12 = [];
c12 = zeros(size(c1));

% HCOOH
c13 = [0.00E+00
0.00E+00
0.00E+00
0.00E+00
0.00E+00
0.00E+00
0.00E+00
0.00E+00
0.00E+00
0.00E+00
0.00E+00
0.00E+00
0.00E+00
```

```
0.00E+00
0.00E+00
0.00E+00
0.00E+00
0.00E+00
0.00E+00
0.00E+00
0.00E+00
0.00E+00
0.00E+00
0.00E+00
0.00E+00
0.00E+00
0.00E+00
0.00E+00
0.00E+00
0.00E+00
0.00E+00
0.00E+00
0.00E+00
0.00E+00
0.00E+00
0.00E+00
0.00E+00
0.00E+00
0.00E+00
0.00E+00
0. 00E+00
];

% HCHO
c14 = [-10.1341461
0.041971672
-7.59833E-05
2.42737E-07
-3.39447E-10
2.86342E-13
-1.50893E-16
4.71901E-20
-6.63211E-24
-6.6525E-28
4.14164E-31
-5.16487E-35
-2.43008E-39
1.29426E-42
-1.26793E-46
6.04954E-51
-4.28311E-54
1.65922E-57
-1.03984E-61
-5.54848E-65
1.05397E-68
-9.31734E-73
1.53711E-76
2.07297E-80
-9.61896E-84
2.72572E-88
4.98642E-92
-1.36118E-95
```

```
3.9002E-99
-2.0429E-103
1.1528E-106
-1.6449E-110
-4.8232E-115
-1.1799E-118
-9.3638E-122
1.569E-125
2.9065E-129
-4.5808E-133
4.6483E-137
-1.1123E-140
8. 2768E-145
];

c(:,1) = c1;
c(:,2) = c2;
c(:,3) = c3;
c(:,4) = c4;
c(:,5) = c5;
c(:,6) = c6;
c(:,7) = c7;
c(:,8) = c8;
c(:,9) = c9;
c(:,10) = c10;
c(:,11) = c11;
c(:,12) = c12;
c(:,13) = c13;
c(:,14) = c14;

%%% Constants
n_rpa = [72.8214388
37.9670093
25.8750050
13.2435508
4.1952252
3.2617659
0.3150009
0.2890471
0.0030233
0.0023386
0.0015356
0.0007747
0.0004715
0. 0001858
];

n_gb = [72.427
24.565
18.5404
2.3446
0.7857
0.5924
0.2677
0.2014
0.0253
0.0192
0.0086
0.0066
```

```matlab
0.0003
0. 0002
];

%%% Variables
deltarH = -20592.7525;      %LHS - temp set to answer
deltarH = abs(deltarH);
Tc_rpa = 3367.124;          %RPA Tc calc
Tc_excel = 3383.5;
Tc = 100;
maxTc = 4000;
stepTc = 100;
stepTcMid = 1;
stepTcTrace = 0.1;
sumDiffHn = 0;

%iterators and exit conditions
n = zeros(NG,1);
maxMoles = 122.3984;        %122.3894 = total moles of reactants
limitMoles = 2 * maxMoles;  %limits the number of iters for loops
stepTrace = 0.0001;
stepMin = stepTrace / 10;
stepMid = 0.001;                    %OH thru O includes dissociations
stepMain = 0.1;                     %H2O thru CO2
rangeMain = 5;
rangeMid = 0.1;
rangeTrace = 0.01;

flag = 0;
poly = zeros(ROWS,COLS);
solns = [];
TcVect = [];
maxSolns = 100000;
sndex = 0;
pn = zeros(NG,1);                   %%previous mole amount temp variable
counter = 0;

while Tc <= maxTc
    low = deltarH - rangeMain;
    high = deltarH + rangeMain;
    n = zeros(NG,1);        %reset moles vector

    for i=1:ROWS
        for j=1:COLS
            poly(i,j) = c(i,j) * (Tc^p(i));
        end
    end

    diffH = zeros(NG,1);
    for i=1:NG
        diffH(i) = sum(poly(:,i));
    end

    %%%% Calc 1st 2 major species
    block = 2; %loop depth and set block size sw =
    0;

    while sumDiffHn < low && (n(1) < maxMoles)  %%H2O
```
115

```matlab
        if sw == 0
            if sumDiffHn < deltarH -1000
                n(1) = n(1) + 4;
            else
                n(1) = n(1) + stepMain;
            end
        end

        %%% H calcs
        diffHn = zeros(COLS,1);
        for i=1:COLS
            diffHn(i) = n(i) * diffH(i);
        end
        sumDiffHn = sum(diffHn);
    end  %%H2O

%        n
%         sumDiffHn

    while sumDiffHn < deltarH && sum(n) < limitMoles %%CO
        %%% H calcs
        diffHn = zeros(COLS,1);
        for i=1:COLS
            diffHn(i) = n(i) * diffH(i);
        end

        sumDiffHn = sum(diffHn);

        if sumDiffHn < deltarH-1000
            n(2) = n(2) + 4;
        else
            n(2) = n(2) + stepMain;
        end

        if sumDiffHn > low
            n(1) = n(1) - n(2);
        end
                 %   H calcs
        diffHn  =  zeros(COLS,1);
        for i=1:COLS
            diffHn(i) = n(i) * diffH(i);
        end

        sumDiffHn = sum(diffHn);
    end  %%CO

%        n
%         sumDiffHn

    n(3) = n_gb(3);
    n(1) = n(1) - n(3);
    sumDiffHn = calcHn(diffH, n, COLS);

     while sumDiffHn < deltarH && sum(n) < limitMoles      %%H2

        %%% H calcs
        sumDiffHn = calcHn(diffH, n, COLS);
```

```matlab
        if sumDiffHn < deltarH-1000
            n(3) = n(3) + 3;
        else
            n(3) = n(3) + stepMain;
        end

        if sumDiffHn > low
            n(1) = n(1) - n(3);
        end

        %%% H calcs
        sumDiffHn = calcHn(diffH, n, COLS);
        %n
    end  %%H2

%           n
%           sumDiffHn

    n(4) = n_gb(4);
    n(1) = n(1) - 5*n(4);
    n(2) = n(2) - 2*n(4);
    sumDiffHn = calcHn(diffH, n, COLS);

     while sumDiffHn < deltarH && sum(n) < limitMoles      %%CO2

        %%% H calcs
        sumDiffHn = calcHn(diffH, n, COLS);

        if sumDiffHn < deltarH-100
            n(4) = n(4) + 3;
        else
            n(4) = n(4) + stepMain;
        end

        if sumDiffHn > low-100
            n(1) = n(1) - n(4);
            n(2) = n(2) - n(4);
        end

        %%% H calcs
        sumDiffHn = calcHn(diffH, n, COLS);
        %n
    end  %%CO2

%           n
%           sumDiffHn

    n(5) = n_gb(5);
    n(2) = n(2) - 5*n(5);
    n(3) = n(3) - n(5);
    n(4) = n(4) - n(5);
    sumDiffHn = calcHn(diffH, n, COLS);

     while sumDiffHn < deltarH && sum(n) < limitMoles      %%OH

        %%% H calcs
```

117

```matlab
        sumDiffHn = calcHn(diffH, n, COLS);

        if sumDiffHn < deltarH-100
            n(5) = n(5) + 2;
        else
            n(5) = n(5) + stepMain;
        end

        if sumDiffHn > low-100
            n(2) = n(2) - n(5);
        end

        %%% H calcs
        sumDiffHn = calcHn(diffH, n, COLS);
    end  %%OH

%          n
%           sumDiffHn

    n(6) = n_gb(6);
    n(5) = n(5) - 2*n(6);
    sumDiffHn = calcHn(diffH, n, COLS);

     while sumDiffHn < deltarH && sum(n) < limitMoles      %%H

        %%% H calcs
        sumDiffHn = calcHn(diffH, n, COLS);

        if sumDiffHn < deltarH-10
            n(6) = n(6) + 3;
        else
            n(6) = n(6) + stepMain;
        end

        if sumDiffHn > low
            n(5) = n(5) - n(6);
        end

        %%% H calcs
        sumDiffHn = calcHn(diffH, n, COLS);
    end  %%H

%          n
%           sumDiffHn

    low = deltarH - rangeMid;
    high = deltarH + rangeMid;
    n(7) = n_gb(7);
    n(1) = n(1) - stepMain;
    n(4) = n(4) - n(7);
    n(5) = n(5) - 5*n(7);
    sumDiffHn = calcHn(diffH, n, COLS);

     while sumDiffHn < deltarH && sum(n) < limitMoles      %%O2

        %%% H calcs
        sumDiffHn = calcHn(diffH, n, COLS);
```

118

```matlab
        if sumDiffHn < deltarH
            n(7) = n(7) + stepMain;
        else
            n(7) = n(7) + stepMid;
        end
        %%% H calcs
        sumDiffHn = calcHn(diffH, n, COLS);
    end %%O2

%        n
%        sumDiffHn


    n(8) = n_gb(8);
    n(5) = n(5) - n(8);
    sumDiffHn = calcHn(diffH, n, COLS);

    while sumDiffHn < deltarH && sum(n) < limitMoles      %%O

        %%% H calcs
        sumDiffHn = calcHn(diffH, n, COLS);

        if sumDiffHn < deltarH-1
            n(8) = n(8) + stepMain;
        else
            n(8) = n(8) + stepMid;
        end
        %%% H calcs
        sumDiffHn = calcHn(diffH, n, COLS);
        if sumDiffHn > low
            n(6) = n(6) - n(8);
        end
    end  %%O

%        n
%        sumDiffHn


    n(9) = stepMid;
    sumDiffHn = calcHn(diffH, n, COLS);

    while sumDiffHn < low && sum(n) < limitMoles    %%HCO

        %%% H calcs
        sumDiffHn = calcHn(diffH, n, COLS);

        if sumDiffHn < deltarH-10000
            n(9) = n(9) + stepMid;
        else
            n(9) = n(9) + stepTrace;
        end
        %%% H calcs
        sumDiffHn = calcHn(diffH, n, COLS);
        if sumDiffHn > deltarH
            n(8) = n(8) - n(9);
        end
```

119

```matlab
    end  %%HCO

%         n
%         sumDiffHn

    n(10) = stepMid;
    n(9) = n(9) - 10*n(10);
    sumDiffHn = calcHn(diffH, n, COLS);

     while sumDiffHn < low && sum(n) < limitMoles     %%HO2

        %%% H calcs
        sumDiffHn = calcHn(diffH, n, COLS);

        if sumDiffHn < low-1000
            n(10) = n(10) + stepMid;
        else
            n(10) = n(10) + stepTrace;
        end
        %%% H calcs
        sumDiffHn = calcHn(diffH, n, COLS);
        if sumDiffHn >= low
            n(9) = n(9) - n(10);
        end
    end  %%HO2
    %n
    %sumDiffHn

    %%%%%%%%%%%%%%%%%%%%%%%%%%%
    %   IMPORTANT
    %   THE CHANGE IN ENTHLAPY IS 0
    %   HENCE WHY 11 THRU 13 CALCUATIONS WON'T WORK!!!
    %  using GB instead
    %%%%%%%%%%%%%%%%%%%%%%%%%%
    n(11:13) = n_gb(11:13);
    n(9) = n(9) - n(10) - n(11) - n(12) - n(13);    %update n(9)


%         n(11) = stepMid;
%         sumDiffHn = calcHn(diffH, n, COLS);
%         while sumDiffHn < low-1 && sum(n) < limitMoles     %%COOH
%
%             %%% H calcs
%             %sumDiffHn = calcHn(diffH, n, COLS);
%
%             %if sumDiffHn < low-1000
%             %    n(11) = n(11) + stepMid;
%             %else
%                 n(11) = n(11) + 10;
%             %end
%             %%% H calcs
%             %n
%             sumDiffHn = calcHn(diffH, n, COLS);
%             if sumDiffHn >= deltarH
%                 n(9) = n(9) - n(11);
%             end
%             %disp('fire 11')
%             %n
```

120

```matlab
%        end   %%COOH
%        n
%        sumDiffHn

%        n(12) = stepTrace;
%        n(8) = n(8) - n(12);
%        sumDiffHn = calcHn(diffH, n, COLS);
%
 %          while sumDiffHn < deltarH && sum(n) < limitMoles     %%H2O2
 %
 %              %%% H calcs
 %              sumDiffHn = calcHn(diffH, n, COLS);
 %
 %              if sumDiffHn < low
 %                  n(12) = n(12) + stepTrace;
 %              else
 %                  n(12) = n(12) + stepMin;
 %              end
 %              %%% H calcs
 %              sumDiffHn = calcHn(diffH, n, COLS);
 %              if sumDiffHn > low
 %                  %n(7) = n(7) - n(12);
 %              end
 %              %disp('asdf')
 %              %n
%        end   %%H2O2
%        n
%        sumDiffHn
%
%        n(13) = stepTrace;
%        n(8) = n(8) - n(13);
%        sumDiffHn = calcHn(diffH, n, COLS);
%
 %          while sumDiffHn < deltarH && sum(n) < limitMoles     %%HCOOH
 %
 %              %%% H calcs
 %              sumDiffHn = calcHn(diffH, n, COLS);
 %
 %              if sumDiffHn < low
 %                  n(13) = n(13) + stepTrace;
 %              else
 %                  n(13) = n(13) + stepMin;
 %              end
 %              %%% H calcs
 %              sumDiffHn = calcHn(diffH, n, COLS);
 %              if sumDiffHn > low
 %                  %n(7) = n(7) - n(13);
 %              end
 %              %disp('asdf')
 %              %n
%        end   %%HCOOH
%        n
%        sumDiffHn


    %n(14) = stepTrace;
    n(14) = n_gb(14);
    n(1:NG-1) = n(1:NG-1) - n(14);
    sumDiffHn = calcHn(diffH, n, COLS);
```

```matlab
%
%           while sumDiffHn < deltarH && sum(n) < limitMoles     %%HCHO
%
%               %%% H calcs
%               sumDiffHn = calcHn(diffH, n, COLS);
%
%               if sumDiffHn < low
%                   n(14) = n(14) + stepTrace;
%               else
%                   n(14) = n(14) + stepMin;
%               end
%               %%% H calcs
%               sumDiffHn = calcHn(diffH, n, COLS);
%               if sumDiffHn > low
%                   %n(3) = n(3) - n(14);
%               end
%           end  %%HCHO

%           n
%           sumDiffHn
%           errSumH = abs((deltarH - sumDiffHn) / deltarH)


    if Tc <=  3000
        Tc = Tc  + stepTc;
     elseif Tc > 3000 && Tc < 3300
        Tc = Tc  + stepTcMid;
     elseif Tc >= 3300 && Tc < 3400
        Tc = Tc  + stepTcTrace;
     elseif Tc >= 3400 && Tc <= 4000
         Tc = Tc + stepTcMid;
    else
        Tc = Tc  + stepTcMid;
    end
    %Tc = Tc + 0.225 * sqrt(Tc); %another method to update Tc Tc


    if abs(sumDiffHn - deltarH) < 10
        solns = [solns n];
        TcVect = [TcVect Tc];
    end
end

%%%%%%%%%%%%%%%%%%%%%%%%%%%%%%%%%%%%%%%%%%%%%%%%%%%%%%%%%%%%%%
% Compre Results
%%%%%%%%%%%%%%%%%%%%%%%%%%%%%%%%%%%%%%%%%%%%%%%%%%%%%%%%%%%%%%
[ms ns] = size(solns);
err = zeros(1,NG); prev
= err;
solndex = 1;

for i=1:ns
    prev = err;
    avgPrev = 0;
    avg = 0;
    negFlag = 0;

    for j=1:NG
```

122

```
        err(j) = abs((solns(j,i) - n_rpa(j)) / n_rpa(j));

        if solns(j,i) < 0
            negFlag = 1;
        end
    end
    avg = sum(err);
    avgPrev = sum(prev);


    totalErr = abs((sum(solns(:,i)) - sum(n_rpa)) / sum(n_rpa));
    tempErr = abs((TcVect(i) - Tc_rpa) / Tc_rpa);

    if (totalErr < 0.001) && (tempErr < 0.001) && (negFlag == 0)
        if avg < avgPrev
            solndex = i;
        end
    end
end

tcndex = 0;
tcErr = 0;
for i=1:ns
    tcPrev = tcErr;
    tcErr = abs((TcVect(i) - Tc_excel) / Tc_excel);

    if TcVect == Tc_ rpa
        tcndex = i;
    elseif tcErr < tcPrev
        tcndex = i;
    end
end

solns(:, solndex)
TcVect(solndex)

solns(:, tcndex)
TcVect(tcndex)
```

Acknowledgements